

NEURAL-NETWORK-BASED REGULARIZATION METHODS FOR INVERSE PROBLEMS IN IMAGING

ANDREAS HABRING AND MARTIN HOLLER

ABSTRACT. This review provides an introduction to - and overview of - the current state of the art in neural-network based regularization methods for inverse problems in imaging. It aims to introduce readers with a solid knowledge in applied mathematics and a basic understanding of neural networks to different concepts of applying neural networks for regularizing inverse problems in imaging. Distinguishing features of this review are, among others, an easily accessible introduction to learned generators and learned priors, in particular diffusion models, for inverse problems, and a section focusing explicitly on existing results in function space analysis of neural-network-based approaches in this context.

CONTENTS

1. Introduction	1
2. Notation	5
3. Unsupervised Models	6
4. Supervised	20
5. Untrained Models	24
6. Function Space Analysis of Neural-network-based Approaches	30
7. Quantifying Uncertainty in Learned Models	34
References	36

1. INTRODUCTION

The field of inverse problems in imaging is probably among the mathematical fields that were most affected by the rise of neural-network-based deep learning techniques of the past decade. Accounting for this, the present article strives to provide an overview of the current state of the art regarding techniques to solve inverse problems in imaging under the use of neural networks (NNs), in particular convolutional neural networks (CNNs). Its main focus is to explain the most successful approaches conceptually and, thus, enable a clear understanding of the discussed methods rather than provide an exhaustive literature review. In order to facilitate a concise presentation, details regarding notation and precise mathematical definitions are kept to a minimum, and readers are assumed to have a good basis in applied mathematics and to be already familiar with the notion of neural networks

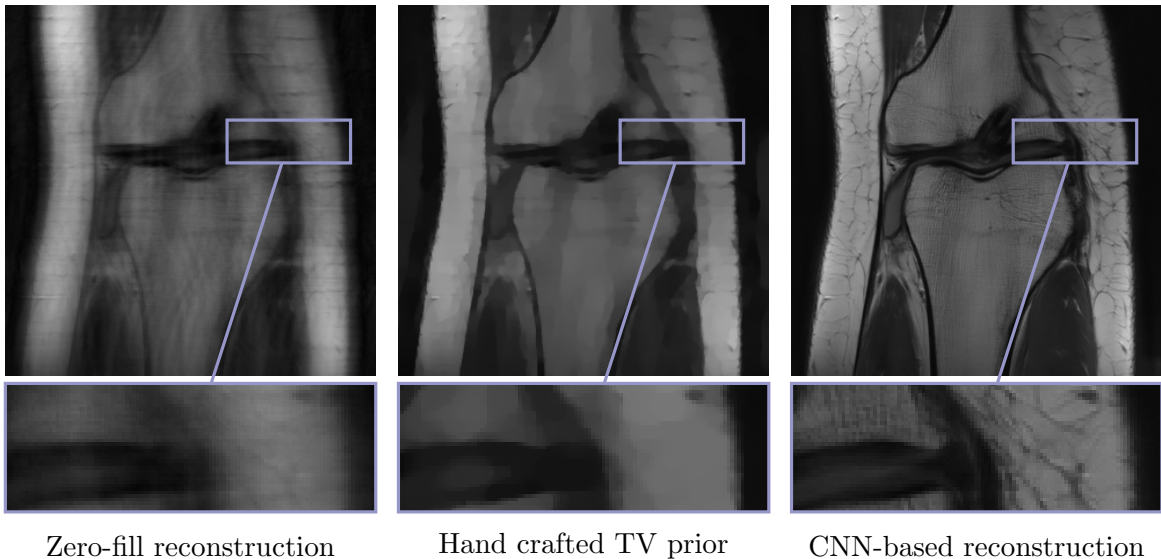


FIGURE 1. Comparison of different methods for the reconstruction of magnetic resonance images from subsampled data. From left to right: Reconstruction by setting unknown data components to zero, classical variational approach with TV prior [158], result of trained, neural-network based reconstruction approach from [83], see also [206]¹. Data taken from [112].

in general. Furthermore, we emphasize already at this point that, given the size and rapid development of the field, such a review can of course never be complete and we refer readers also to other reviews listed in Section 1.1 below for a more comprehensive overview.

In inverse problems in imaging, the goal is to infer an unknown ground truth signal $u \in \mathcal{X}$ (usually an image) given a measurement or observation $y \in \mathcal{Y}$. Ground truth and observation are related to each other via the so-called forward operator $A : \mathcal{X} \rightarrow \mathcal{Y}$ according to

$$(1) \quad y = Au + \zeta,$$

where ζ denotes possible measurement noise (we consider additive noise here for simplicity, but the noise might, e.g., also be multiplicative). In many cases of interest such as magnetic resonance imaging (MRI), computed tomography (CT), electrical impedance tomography (EIT) or super-resolution the forward operator is, in fact, not invertible or its inverse is (severely) ill-conditioned, rendering (1) an ill-posed problem. A popular remedy to overcome ill-posedness are variational regularization methods [162, Section 3] where, as a surrogate for (1), one aims to solve

$$(2) \quad \min_u \mathcal{D}_y(Au) + \lambda \mathcal{R}(u)$$

¹The authors thank Martin Zach from Graz University of Technology for providing these results.

where $\mathcal{D}_y(Au)$ denotes a data fidelity term ensuring $Au \approx y$, such as, e.g., $\mathcal{D}_y(Au) = \frac{1}{2} \|Au - y\|_2^2$. The functional \mathcal{R} denotes a regularizer which ensures that (2) is well-posed, i.e., it admits a solution which depends continuously on the data [162, Section 3.1]. An example highly popular in particular in imaging problems is the total variation functional (TV) [158, 9], which reads as $\mathcal{R}(u) = \text{TV}(u) = \|\nabla u\|_1$ in the discrete setting.

Especially in the context of data-driven approaches, a Bayesian perspective of (1) is often adopted. In this case u, y, ζ are modeled as random variables, with u, y having a joint distribution $p(u, y)$, and one considers the log of the *posterior* distribution of u after observing y , which can be computed using Bayes' theorem as

$$(3) \quad -\log p(u|y) = -\log p(y|u) - \log p(u) + \log p(y).$$

We call $p(y|u)$ the data likelihood and $p(y)$ the prior distribution. As is common in machine learning literature, as long as there is no risk of ambiguity, we simply use the letter p to denote any probability density and specify the exact density only through the input argument, e.g., $p(u)$ denotes the density of the ground truth u . Note that (3) allows for point estimation of u via computing the maximum a-posteriori (MAP) estimate, that is, the value of u maximizing $p(u|y)$. On the other hand, Markov chain Monte Carlo (MCMC) methods such as the unadjusted Langevin algorithm and its variations [63, 62, 64, 118, 80] allow for sampling from $p(u|y)$. Thus, instead of the MAP, we can as well compute the expected value of $p(u|y)$ called the MMSE or, for that matter, any other statistic of the posterior such as the variance [137, 207, 206].

If we identify the distributions occurring in (3) as the Gibbs measures

$$p(y|u) \propto \exp(-\mathcal{D}_y(Au)) \quad \text{and} \quad p(u) \propto \exp(-\mathcal{R}(u)),$$

we find an equivalence of variational regularization and Bayesian modeling, which is why a strong distinction between the two approaches is not necessary in many cases and we will frequently discuss, e.g., models for $p(u)$ while keeping in mind that this is equivalent to models of $\mathcal{R}(u)$.

While the modeling of $p(y|u)$ is mostly a question of obtaining appropriate forward and noise models (which is an important research direction on its own), the prior distribution, respectively regularizer, has been subject to a lot of research in particular in inverse imaging problems, with popular examples being Tikhonov regularization [68, Section 5], total variation regularization [158] and its generalization to higher-order approaches [33, 32]. As a consequence of the high complexity of image data, hand crafted methods for solving inverse problems seemed to reach a limit in terms of empirical performance. However, in the past decades, data driven approaches were able to significantly push forward the boundaries of reconstruction quality with appropriate priors. An illustrative example in this context is provided in Figure 1, where the performance of the hand crafted TV prior [158] is compared to the performance of the neural-network based approach of [83] for subsampled MRI.

In this article we focus our attention specifically on data driven methods utilizing NNs. While there exist other regimes, the presented methods focus on the case that the forward operator A is known and will be classified in three different categories: i) unsupervised methods, where during training we require only a sample $(u_i)_i$ of images from the prior

distribution $p(u)$ (Section 3), ii) supervised methods, where during training we use a sample $(u_i, y_i)_i$ of image-observation pairs from the joint distribution $p(u, y)$ (Section 4), and iii) untrained methods, where NNs are used without any prior training (Section 5). This terminology slightly deviates from the conventional one in machine learning literature in the sense that in the context of inverse problems the goal is to predict u from y meaning that u , in fact, constitutes the *label* and y the *feature*. Thus, in the classical sense unsupervised would refer to methods training solely on a sample $(y_i)_i$. These approaches are frequently referred to as self-supervised [168, 91, 119, 140] in the context of inverse problems and will not be discussed in detail in the present article. For an overview of the different types of settings, methods and corresponding training strategies considered in this article we refer to Table 1.

After providing an overview of NN based machine learning approaches within these three categories, we further discuss the state of the art in this area in terms of function space modeling (Section 6) and uncertainty quantification (Section 7).

1.1. Relation to Existing Review Articles. Given the importance of the field, naturally there exist several different, also rather recent review articles on topics related to the scope of this work. Nevertheless, we believe the present article, with a clearly defined scope and a focus on presenting methods, concepts, and mathematical aspects rather than listing existing works, provides an additional contribution. In particular, we believe that some of the unique features of the present article are i) the focus on neural-network based methods for inverse problems in imaging, which allows a comprehensive yet rather detailed, method-driven introduction to the field, ii) a fairly detailed, self-contained summary of the state of the art in using learned generators and learned priors for inverse problems in imaging (see Sections 3.1 and 3.2), including in particular score based models and diffusion models, and iii) the inclusion of a section focused on existing results in function space analysis (see Section 6), which is an important topic in classical inverse problems literature. It is also worth mentioning that the field of deep learning is still evolving rapidly, such that review articles become outdated already after five years or less. This allows the present article to provide a contribution also compared older articles, even if they have a very similar scope.

Nevertheless, many excellent, recent review article exist that cover important aspects that are also in the focus of this work. The following paragraph lists some of them, and we recommend the interested reader to consult them in particular either for a more in-depth treatment of some topics mentioned here only briefly, or to get a larger picture including aspects of neural-network based methods for inverse problems in imaging that are not covered here.

A review article on data-driven methods that is already classical in the mathematical inverse problems community is the comprehensive work [17]. Here, the scope is more general than the one of our work, however, due to the appearance of [17] in 2019, important parts in particular of Sections 3.1 and 3.2 are not covered in the same depth as in the present article.

The scope of [140] is probably closest to the scope of our work. In [140] a taxonomy to categorize different problems and reconstruction methods in the context of deep learning

for inverse problems, depending on the extent to which the forward model is known or unknown is presented. Differences to our work are, for instance, that the recency of our work allowed us provide more details on concepts and methods such as score based models, diffusion models and function space theory.

The very recent review [135] focuses in particular on methods with convergence guarantees. It has intersections in particular with Section 6 of our work, but does not cover topics such as learned generators and learned priors (see Sections 3.1 and 3.2) in the same depth as we do.

The review paper [161] is focused on a theoretical perspective of deep learning, in particular in a compressed sensing context, and puts most emphasis on generator-based models and untrained approaches. The work [28] in turn provides a review focused on mathematical aspects of deep learning in general, such as approximation results, generalization, and optimization aspects.

A related review is further [171], which focuses on model-based deep learning, in particular on the three topics of learning model-based optimization algorithms, unfolding optimizers into trainable architectures (cf. Section 4.3), and the augmentation of model-based algorithms with trainable neural networks.

Further reviews very much related to the scope of our work are [129, 124]. Due to their appearance in 2017 and 2018, however, they naturally do not fully cover the state of the art in this rapidly evolving field anymore.

Another relevant review is [25] which, compared to our work, is probably less method-driven, and again does not cover important parts of the works we discuss in Sections 3.1 and 3.2.

For a recent review paper on uncertainty quantification in deep learning in general, we refer to [1] and for a more extensive review on generator-based regularization for inverse problems see [60]

Finally, the works [121, 209] provide reviews of deep learning methods in the context of medical imaging.

2. NOTATION

Part of our notation was already introduced in the introduction, and due to the nature of this work, we strive to use notation in a way allowing the educated reader to easily follow our elaborations without the necessity of precise definitions and details.

As already mentioned, the forward model in this article will always be denoted by $A : \mathcal{X} \rightarrow \mathcal{Y}$, where \mathcal{X} is the space of images and \mathcal{Y} is the measurement or observations space, which is not necessarily an image space (cf. MRI). Most of the methods in this article regard \mathcal{X} and \mathcal{Y} to be finite dimensional vector spaces; the function space settings will only play a role in Section 6. Also, for the sake of simplicity and since our focus is on the regularization rather than the forward model, A will always be assumed to be linear unless explicitly stated otherwise.

Neural networks will usually be denoted as \mathcal{N}_θ , where θ summarizes the network parameters usually consisting of weights (or convolution kernels) w and biases b , i.e., $\theta = (w, b)$.

Depending on the method at hand, networks will for example map from images space to \mathbb{R} , i.e., $\mathcal{N}_\theta : \mathcal{X} \rightarrow \mathbb{R}$, from latent space to image space, i.e., $\mathcal{N}_\theta : \mathcal{Z} \rightarrow \mathcal{X}$, where \mathcal{Z} and z usually denote the latent space and latent variables, respectively, or from image space to image space $\mathcal{N}_\theta : \mathcal{X} \rightarrow \mathcal{X}$. We assume the reader to be familiar with the general architecture of neural networks, and refer for instance to [28] for a precise, mathematical definition.

Setting	Method	Parameter fitting strategy
Unsupervised	Learned generator	Maximum likelihood
		Autoencoder
		VAE
		GAN
	Learned prior	Maximum likelihood
		Score-matching and diffusion models
		Plug and Play
RED	Pre-trained denoiser	
Supervised	Fully learned	Minimal reconstruction error
	Post-processing	Minimal reconstruction error
		GAN
	Unrolling	Minimal reconstruction error
	Learned prior	Minimal reconstruction error
Adversarial regularizer		
Untrained	Generator-network	Approximate observed data

TABLE 1. Overview over the methods discussed in this article.

3. UNSUPERVISED MODELS

We start this survey by considering unsupervised methods, that is, we assume access to an independent and identically distributed (iid) data set $(u_i)_{i=1}^N$ of images following the prior distribution $p(u)$. The first two subsections Sections 3.1 and 3.2 elaborate on approaches for training an approximate model of $p(u)$, respectively $\mathcal{R}(u)$ such that $p(u) \propto \exp(-\mathcal{R}(u))$. After we have access to such a model, the ground truth u for a new observation y can be estimated either by minimizing (3) or by sampling from the posterior $p(y|u)$ as explained in the introduction. Then, in Sections 3.3 and 3.4, we will discuss Plug and Play approaches and regularization by denoising. In the former, generic denoisers are

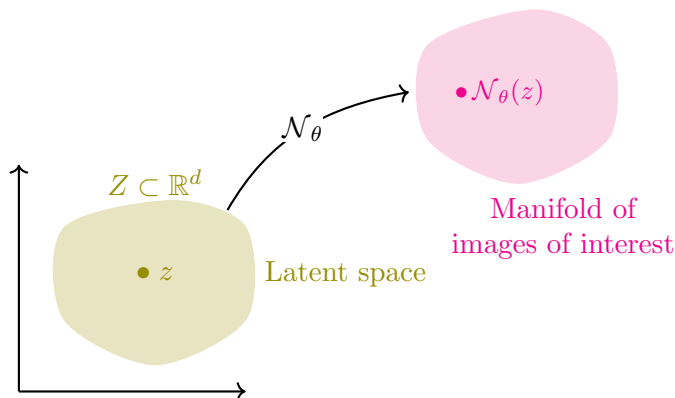


FIGURE 2. Illustration of a learned generator.

used in place of the proximal mapping $\text{prox}_{\mathcal{R}}(u) := \arg \min_v \frac{\|u-v\|_2^2}{2} + \mathcal{R}(v)$ appearing in optimization algorithms, and in the latter denoisers replace the gradient $\nabla \mathcal{R}$, such that MAP estimation or inference based on $p(u|y)$ is possible without knowing \mathcal{R} explicitly.

3.1. Learned Generators. In this article *learned generators* refers to models where one aims to learn a parametrization of the manifold of images of interest, cf. Figure 2. More precisely, given a tractable latent distribution $p(z)$, e.g., a Gaussian distribution, a model \mathcal{N}_θ is trained such that for $z \sim p(z)$ it holds $\mathcal{N}_\theta(z) \sim p(u)$. That is, the network pushes the latent distribution forward to the image distribution. In that sense, $p(u)$ is not learned explicitly, but rather implicitly via the parametrization \mathcal{N}_θ . Employing this parameterization, the inverse problem (1) is transferred to

$$(4) \quad y = A \mathcal{N}_\theta(z) + \zeta,$$

and we find for the posterior distribution of the latent variable

$$(5) \quad -\log p(z|y) = -\log p(y|z) - \log p(z) + \text{const.}$$

In particular, in the case of Gaussian noise $\zeta \sim \mathcal{N}(0, \sigma^2)$ and a Gaussian distribution on the latent space $z \sim \mathcal{N}(0, 1)$ we obtain

$$(6) \quad -\log p(z|y) = \frac{1}{2\sigma^2} \|A \mathcal{N}_\theta(z) - y\|_2^2 + \frac{1}{2} \|z\|_2^2 + \text{const.}$$

Consequently, (6) allows to apply a learned generator in a variational as well as a Bayesian setting. A crucial degree of freedom in such methods utilizing a learned generator is the approach for training \mathcal{N}_θ , for which a maximum likelihood estimation, generative adversarial networks (GAN), or (variational) autoencoders (VAE) are applicable.

3.1.1. Maximum Likelihood Estimation. In order to perform maximum likelihood estimation, we first need to obtain an explicit formulation for the likelihood induced by the generator. This, however, can only be achieved if the generator \mathcal{N}_θ is a diffeomorphism, that is, continuously differentiable and invertible with continuously differentiable inverse

[111, 57, 56, 106]. This poses extensive constraints on the architecture, in particular, prohibiting the use of ReLU activations and imposing restrictions on linear/convolutional layers of the network. Performing a change of variables, we find for p_θ the distribution of $\mathcal{N}_\theta(z)$

$$(7) \quad p_\theta(u) = p(z) |D\mathcal{N}_\theta^{-1}(u)|$$

where $z = \mathcal{N}_\theta^{-1}(u)$ and $D\mathcal{N}_\theta^{-1}$ denotes the Jacobian of \mathcal{N}_θ^{-1} . Such models, transforming a complicated distribution to a tractable one via a composition of invertible mappings, e.g., an invertible neural network, are referred to as *normalizing flows* in the literature [111, 150]. Given an iid sample of images following the prior distribution $(u_i)_{i=1}^N$, $u_i \sim p(u)$, the explicit expression for p_θ allows to pursue maximum likelihood estimation of the parameters θ by solving

$$(8) \quad \arg \max_{\theta} \sum_{i=1}^N \log p_\theta(u_i).$$

An application of normalizing flows for inverse problems as explained can be found in [18]. Another related approach to employ normalizing flows to inverse problems is to train the flow directly as a parametrization of the posterior $p(u|y)$ rather than the prior [180, 152, 194]. Note, however, that these methods assume an already given prior distribution $p(u)$. Thus, one either has to rely on a handcrafted or a separate pre-trained prior. On the other hand, it is possible to learn a *conditional normalizing flow*, that is, a network with inputs z and y such that for a fixed y it holds that $\mathcal{N}_\theta(y, z) \sim p(u|y)$ for $z \sim p(z)$. Training such a conditional flow, however, typically leads to a supervised approach [195, 172].

3.1.2. Autoencoders. In the case of autoencoders [139], we aim to find two transformations, an encoder $E_\phi : \mathcal{X} \rightarrow \mathcal{Z}$ which maps images to latent variables and a decoder $D_\theta : \mathcal{Z} \rightarrow \mathcal{X}$ which, in reverse, maps latent variables to images. Subsequently, the decoder is used as the learned generator. In practice, usually the latent space is chosen low-dimensional compared to the image space, $\dim(\mathcal{Z}) \ll \dim(\mathcal{X})$, which acts as a regularization [139]. We wish to find parameters (ϕ, θ) of encoder and decoder such that $D_\theta \circ E_\phi(u) \approx u$ for any image from our distribution $p(u)$. Thus, the corresponding training problem reads, e.g., as

$$(9) \quad \arg \min_{\theta, \phi} \frac{1}{N} \sum_{i=1}^N \ell(D_\theta(E_\phi(u_i)), u_i)$$

where $\ell(\cdot, \cdot)$ denotes some loss functional, e.g., the MSE loss $\ell(u, v) = \frac{1}{2} \|u - v\|_2^2$. Of course adding regularization of the parameters (ϕ, θ) , e.g., via penalizing their norms in (9) is possible and reasonable to ensure well-posedness of the training problem.

3.1.3. Variational Autoencoders. While in practice variational autoencoders (VAE) [110] are implemented using a decoder and an encoder network in a similar fashion to *non-variational* autoencoders, the underlying mathematical formulations of the two differ significantly. Again, our goal is to determine the parameters θ of a complex distribution $p_\theta(u)$ such that $p_\theta(u) \approx p(u)$. We assume that u depends on the latent variable z . The latent

distribution $p(z)$ of z is modeled as a standard Gaussian. The conditional distribution $p_\theta(u|z)$, on the other hand, is chosen as a multivariate Gaussian with mean and covariance μ_z and Σ_z , which are functions of z , both modeled as neural networks with parameters θ . That is, in this case the neural networks map the latent variable z to the parameters of a distribution and not to a data point. The variance Σ_z is frequently restricted to be a diagonal matrix which reduces complexity significantly [110, Appendix C.2]. In subsequent computations we will also make use of the distribution of $z|u$. However, since this distribution is not tractable in general based on the model $p_\theta(u|z)$ we approximate it with a second model $q_\phi(z|u)$. As for $p_\theta(u|z)$, $q_\phi(z|u)$ is modeled as a Gaussian with parameters μ_u and Σ_u , which are neural network functions with parameters ϕ . For training we aim to maximize the log-likelihood (or *evidence*) $\sum_i \log p_\theta(u_i)$ of the model with respect to θ . However, this approach is not directly tractable which is why we employ a lower bound of the likelihood referred to as the evidence lower bound (ELBO) derived as follows:

$$\begin{aligned}
 \log p_\theta(u) &= \log \int p_\theta(u, z) dz = \log \int \frac{p_\theta(u, z)}{q_\phi(z|u)} q_\phi(z|u) dz \\
 &\geq \int \log \left[\frac{p_\theta(u, z)}{q_\phi(z|u)} \right] q_\phi(z|u) dz \\
 (10) \quad &= \mathbb{E}_{z \sim q_\phi(z|u)} [\log p_\theta(u, z) - \log q_\phi(z|u)] \\
 &= \mathbb{E}_{z \sim q_\phi(z|u)} [\log p_\theta(u|z) + \log p(z) - \log q_\phi(z|u)] \\
 &= \mathbb{E}_{z \sim q_\phi(z|u)} [\log p_\theta(u|z)] - \text{KL}(q_\phi(z|u) \| p(z)) \\
 &=: \text{ELBO}(\theta, \phi, u)
 \end{aligned}$$

where we used Jensen's inequality in the second line and $\text{KL}(q \| p) := \int \log\left(\frac{q(z)}{p(z)}\right) q(z) dz$ is the Kullback-Leibler (KL) divergence with $\frac{q(z)}{p(z)}$ the Radon Nikodým derivative for the distributions p, q such that q is absolutely continuous w.r.t p . Given (θ, ϕ, u) , computation of $\text{ELBO}(\theta, \phi, u)$ is feasible and simple since the KL divergence between Gaussians is explicit and sampling from $z \sim q_\phi(z|u)$ is straightforward as well given the Gaussian model. Maximizing the likelihood of the entire iid sample, the parameters are then determined as

$$\arg \max_{\theta, \phi} \sum_{i=1}^N \text{ELBO}(\theta, \phi, u_i)$$

and we refer to [110] for details on the optimization procedure. Note that given our model of p_θ the term $\log p_\theta(u|z)$ within the ELBO reads as

$$(11) \quad \log p_\theta(u|z) = -\frac{\|u - \mu_z\|_2^2}{2\sigma_z^2} + \text{const.}$$

Let us denote the neural network modeling μ_z as $\mu_z = \mathcal{N}_\theta(z)$. Thus, while conceptually \mathcal{N}_θ outputs parameters of a distribution, the fact that during training we maximize (11) shows that \mathcal{N}_θ is trained to reconstruct samples from the target distribution $p(u)$ which

motivates using it as a generator for data points as well. In the following we elaborate on works using VAEs as learned generators.

In [30] Bora et al. apply a generator obtained as the decoder of a VAE (or as the generator of a GAN, see below Section 3.1.4) to compressed sensing by minimizing the posterior (6). They additionally show that under certain conditions the obtained results are close to the ground truth with high probability if the forward operator of the inverse problem is a random Gaussian matrix. Similarly, in [84] a generator from a VAE (and a GAN) is used for the non-linear inverse problem of phase retrieval.

In [20, 19] the authors use generators obtained from VAEs (or GANs, Section 3.1.4) for the solution of blind image deblurring. They use two distinct generators, one for the blur kernel and one for the sought image. In [55] the authors follow a similar approach, however they allow for results with sparse deviations from the range of the generator.

In [71, 61] the authors consider MAP estimation for the posterior of ground truth u and latent variable z , $p_\theta(u, z|y) \propto p(y|u, z)p_\theta(u|z)p(z)$. That is, contrary to the other works, they do not use the VAE as a deterministic mapping $z \mapsto u$ but rather take into account that according to the VAE formulation the generator merely yields distribution parameters. Moreover, in [61] the authors model $\Sigma_z^{-1} = L_z L_z^T$ with L_z a lower triangular matrix with positive diagonal entries. Additionally, sparsity constraints are imposed on L_z .

In [169] it is proposed to solve the inverse problem of electrical impedance tomography with a learned approach in two steps. The authors train an encoder E_{ϕ_1} and a decoder D_{ϕ_2} in a VAE scheme on samples $(u_i)_i$. Afterwards, in a supervised fashion, an additional NN \mathcal{N}_θ is trained to map the the observation to the encoded variables, i.e., $\mathcal{N}_\theta(y_i) \approx E_{\phi_1}(u_i)$. After training, for a new observation y , an estimate of u is then obtained as $u = D_{\phi_2}(\mathcal{N}_\theta(y))$. That is, the prediction method itself is a supervised machine learning method, however, a VAE trained in an unsupervised fashion is used to transfer the problem to latent space (and back).

3.1.4. Generative Adversarial Networks. In the case of generative adversarial networks (GAN) [72] we employ two neural networks during training, a generator G_θ and a discriminator D_ϕ (not to be confused with a decoder) which pursue opposing goals. The generator aims to generate images of the desired target distribution $p(u)$. The discriminator, on the other hand, tries to distinguish samples from the distribution $p(u)$ from samples generated by the G_θ . More precisely, $D_\phi(u)$ yields a number in $[0, 1]$ which represents the estimated probability of its input u being a *real* sample, that is, the discriminator's goal is to predict $D_\phi(u) \approx 1$ for $u \sim p(u)$ and $D_\phi(G_\theta(z)) \approx 0$, whereas the generators goal is to achieve $D_\phi(G_\theta(z)) \approx 1$. A mathematical formulation of the training problem reads, e.g., as

$$(12) \quad \min_{\theta} \max_{\phi} \mathbb{E}_{z \sim p(z)} [\log(1 - D_\phi(G_\theta(z)))] + \mathbb{E}_{u \sim p(u)} [\log(D_\phi(u))].$$

As mentioned above, the works [30, 20, 55, 19, 84] perform their experiments with generators obtained from VAEs as well as from GANs. Specifically, they use the deep convolutional GAN (DCGAN) from [146].

In [170], instead of optimization over the latent space by minimizing $\|A G_\theta(z) - y\|_2^2$ similar to Bora et al. [30], the authors consider solving the constraint minimization problem

$$\arg \min_u \|A u - y\|_2^2, \quad \text{s.t. } u \in \text{Rg}(G_\theta)$$

using projected gradient descent. Here $\text{Rg}(G_\theta) = \{G_\theta(z) \mid z \in \mathbb{R}^n\}$ denotes the range of the generator. In [147] this approach is further modified by replacing the inner loop necessary for the projection onto the range of the generator by a learned projection which is parametrized as an additional neural network.

In [141] the authors use a pre-trained GAN generator and propose to solve

$$(13) \quad \min_{z, \theta} \mathcal{D}_y(A G_\theta(z)),$$

that is, they also allow for additional fine tuning of the parameters of the generator during inference similar to the deep image prior [188], see Section 5. Moreover, as a data fidelity term they use

$$(14) \quad \mathcal{D}_y(u) = \sum_k \|D_\phi(y, k) - D_\phi(A u, k)\|_1$$

where $D_\phi(y, k)$ denotes the k -th layer of the discriminator network.

In [203] the problem of large hole inpainting is tackled using a GAN generator. Instead of the frequently used squared L^2 loss $\frac{1}{2}\|z\|_2^2$ which stems from the standard Gaussian latent distribution model $\log p(z) = -\frac{1}{2}\|z\|_2^2 + \text{const.}$, the authors propose using $\log(1 - D_\phi(G_\theta(z)))$ as a penalty on the latent variable z during MAP estimation.

Wasserstein GAN: It can be shown that (12) amounts to minimizing a specific distance, namely the Jensen-Shannon divergence, between the target density and the density generated by G_θ [72]. In [14] the authors propose to replace the Jensen-Shannon divergence with the Wasserstein-1 distance which improves numerical behavior of the training. Using Kantorovich-Rubinstein duality [191] the resulting training problem reads as

$$(15) \quad \min_\theta \max_{D_\phi \in 1\text{-Lip}} \mathbb{E}_{u \sim p(u)} [D_\phi(u)] - \mathbb{E}_{z \sim p(z)} [D_\phi(G_\theta(z))]$$

where the discriminator D_ϕ is constrained to be Lipschitz continuous with Lipschitz constant 1. This constraint is, however, difficult to enforce strictly, which is why it is commonly relaxed by replacing the discriminator update for a fixed generator with [75]

$$(16) \quad \max_\phi \mathbb{E}_{u \sim p(u)} [D_\phi(u)] - \mathbb{E}_{z \sim p(z)} [D_\phi(G_\theta(z))] - \lambda \mathbb{E}_{\hat{u} \sim p(\hat{u})} [(\|\nabla_u D_\phi(\hat{u})\|_2 - 1)^2]$$

where $p(\hat{u})$ denotes a uniform distribution on straight lines between a sample from $p(u)$ and a sample generated from G_θ . This training strategy, referred to as Wasserstein GAN is, e.g., used in [133] for sampling from the posterior using a GAN for the specific problem of seismic waveform inversion. Wasserstein GANs are also frequently applied in supervised settings and we refer to Section 4.2 for more info.

3.2. Learned Priors. In contrast to the methods in Section 3.1, where the prior is implicitly learned via learning the pushforward from a tractable distribution to $p(u)$, it is also possible to directly approximate the prior, respectively regularizer. An early and prominent example thereof is Fields of Experts (FoE) [156, 157] where the prior is modeled as a product of simple distributions with trainable parameters. In this work, we focus on the approach of parametrizing the regularizer directly as a neural network, i.e., $\mathcal{N}_\theta(u) = -\log p_\theta(u) \approx -\log p(u)$ [207, 206], but note that there exist of course many more subtle approaches such as [8], which trains a patch-based prior using invertible neural networks that is particularly dedicated to limited training data.

A natural approach for directly training a neural network as a regularization functional is the already mentioned maximum likelihood based estimation according to

$$(17) \quad \arg \max_{\theta} \sum_{i=1}^N \log p_\theta(u_i)$$

as pursued in [207, 206, 74, 187] for computed tomography and MRI. It is worth noting that, in the limit for $N \rightarrow \infty$ according to the law of large numbers, maximum likelihood estimation as above is, in fact, equivalent to minimizing the Kullback-Leibler divergence between $p(u)$ and $p_\theta(u)$ if we scale (17) by $\frac{1}{N}$

$$(18) \quad \begin{aligned} \lim_{N \rightarrow \infty} \frac{1}{N} \sum_{i=1}^N \log p_\theta(u_i) &= \mathbb{E}_{u \sim p(u)} [\log p_\theta(u)] \\ &= \mathbb{E}_{u \sim p(u)} [\log p(u)] - \mathbb{E}_{u \sim p(u)} \left[\log \frac{p(u)}{p_\theta(u)} \right] \\ &= -\text{KL}(p(u) || p_\theta(u)) + \text{const.} \end{aligned}$$

3.2.1. Score-based and diffusion models. Maximum likelihood estimation according to (17) is commonly performed using gradient based optimization techniques which require the gradient $\nabla_{\theta} \mathbb{E}_{u \sim p(u)} [\log p_\theta(u)]$. Identifying once again the prior with a learned regularizer via

$$(19) \quad p_\theta(u) = \frac{\exp(-\mathcal{R}_\theta(u))}{\int \exp(-\mathcal{R}_\theta(v)) \, dv}$$

we can compute the gradient using Leibniz's rule for differentiating an integral [206, 92]

$$(20) \quad \nabla_{\theta} \mathbb{E}_{u \sim p(u)} [\log p_\theta(u)] = -\mathbb{E}_{u \sim p(u)} [\nabla_{\theta} \mathcal{R}_\theta(u)] + \mathbb{E}_{u \sim p_\theta(u)} [\nabla_{\theta} \mathcal{R}_\theta(u)].$$

Unfortunately, this reveals a downside of this approach, namely that the second term in (20) is an expected value with respect to $p_\theta(u)$ which is computationally demanding as it has to be approximated using sampling procedures.

Score-based modeling: A remedy is provided by score-based methods: Interestingly, whether we try to compute the MAP via minimizing the variational objective functional or the MMSE estimate via sampling from the posterior, in any case we do not require access to the value of the regularizer, respectively prior, $\log p(u)$ but only its gradient

$\nabla \log p(u)$ called the *score*. This gives rise to a class of methods, referred to as *score-based* modeling, where one aims to directly approximate $\nabla \log p(u)$ using a neural network $s_\theta(u) \approx \nabla \log p(u)$ [97, 174, 175]. The corresponding training problem reads as

$$(21) \quad \min_{\theta} J(\theta) := \mathbb{E}_{u \sim p(u)} \left[\frac{1}{2} \|s_\theta(u) - \nabla \log p(u)\|_2^2 \right].$$

While this functional is not amenable to optimization as we do not have access to $\nabla \log p(u)$, via integration by parts it can be shown [192] that

$$(22) \quad J(\theta) = \mathbb{E}_{u \sim p(u)} \left[\frac{1}{2} \|s_\theta(u)\|_2^2 + \text{tr}(\nabla_u s_\theta(u)) \right] + \text{const.}$$

which can be minimized.

Denoising score matching: In [174], however, the authors argue that direct estimation of the score using samples from $p(u)$ unfortunately suffers from several issues in the case of imaging: It is reasonable to assume, that $p(u)$ is supported in a lower-dimensional manifold rendering the gradient $\nabla \log p(u)$ unamenable. Moreover the estimation of the score will be poor in areas of low probability and lastly, multi-modality of $p(u)$ renders sampling difficult. As a remedy it is proposed to consider smoothing the distribution $p(u)$ with additive Gaussian noise $\tilde{u} = u + \sigma_i \zeta$, $\zeta \sim \mathcal{N}(0, \mathbf{I})$, $0 < \sigma_L < \dots < \sigma_1$ leading to the smoothed distributions $p_{\sigma_i}(\tilde{u}) = p * \mathcal{N}(0, \sigma_i^2 \mathbf{I})(\tilde{u})$, that is, convolutions of $p(u)$ with Gaussians of different variances. For these distributions all the aforementioned issues are reduced. The *noise conditional* score network $s_\theta(\tilde{u}, \sigma_i)$ is then trained to approximate the score $\nabla \log p_{\sigma_i}(\tilde{u})$ for all σ_i , where for $\sigma_i \rightarrow 0$ the desired score should be recovered, by solving

$$(23) \quad \min_{\theta} \sum_{i=1}^L \lambda(\sigma_i) \mathbb{E}_{\tilde{u} \sim p_{\sigma_i}(\tilde{u})} \left[\|s_\theta(\tilde{u}, \sigma_i) - \nabla \log p_{\sigma_i}(\tilde{u})\|_2^2 \right],$$

where λ is a coefficient function allowing to weigh different noise levels differently. As before, due to $\nabla \log p_{\sigma_i}(\tilde{u})$ being unknown, the formulation (23) is unfortunately not amenable to optimization as is. In this case, however, as alternative to (22), the following equivalent problem can be derived [192]:

$$(24) \quad \min_{\theta} \sum_{i=1}^L \lambda(\sigma_i) \mathbb{E}_{u \sim p(u)} \mathbb{E}_{\tilde{u} \sim p_{\sigma_i}(\tilde{u}|u)} \left[\|s_\theta(\tilde{u}, \sigma_i) - \nabla \log_{\tilde{u}} p_{\sigma_i}(\tilde{u}|u)\|_2^2 \right].$$

That is, we can replace the score $\nabla \log p_{\sigma_i}(\tilde{u})$ by the conditional one $\nabla_{\tilde{u}} \log p_{\sigma_i}(\tilde{u}|u)$ which is explicit. Note that by definition of the smoothed distributions, $\nabla_{\tilde{u}} \log p_{\sigma_i}(\tilde{u}|u) = \frac{1}{\sigma_i^2}(u - \tilde{u})$, and, thus,

$$\sigma_i^2 (s_\theta(\tilde{u}, \sigma_i) - \nabla_{\tilde{u}} \log p_{\sigma_i}(\tilde{u}|u)) = (\tilde{u} + \sigma_i^2 s_\theta(\tilde{u}, \sigma_i)) - u$$

showing that $s_\theta(\tilde{u}, \sigma_i)$ is trained to satisfy $(\tilde{u} + \sigma_i^2 s_\theta(\tilde{u}, \sigma_i)) \approx u$, thus, resembling a denoiser.

After the score is trained, sampling using the noise conditional score network is performed using the so-called *annealed Langevin* algorithm [174] which refers to the procedure of consecutively sampling from p_{σ_i} for decreasing noise levels $i = 1, \dots, L$ and for each new

i using the last iterate of the previous Langevin sampling as initialization. That is, we generate Markov chains according to

$$(25) \quad u_i^{k+1} = u_i^k + \gamma_i s_\theta(u_i^k, \sigma_i) + \sqrt{2\gamma_i} \zeta_i^k, \quad k = 0, \dots, K-1$$

where ζ_i^k denote iid standard Gaussian random variables and for $i = 1$ the chain is initialized arbitrarily and for $i > 1$ we use $u_i^0 = u_{i-1}^K$. The step sizes γ_i constitute hyperparameters of the method and can, for instance, be chosen to decrease as the noise scale decreases [174].

Diffusion models: A crucial ingredient in score-based modeling as introduced above is to *corrupt* the target distribution with noise leading to a more well-behaved distribution p_{σ_i} . Afterwards sampling from $p(u)$ is performed by consecutively sampling from p_{σ_i} , $i = 1, \dots, L$. In other words, *we start at a noisy distribution and successively remove the noise from the samples until the target distribution is obtained*. This approach is amenable for generalization. Let us define the noise corruption process starting at the target distribution $p(u)$ and leading to the well-behaved distribution as the following Markov chain

$$(26) \quad u_{i+1} = \alpha_i u_i + \beta_i \zeta_i, \quad i = 0, \dots, L-1$$

with $u_0 \sim p(u)$. By choosing $\alpha_i = 1$, $\beta_i = \sqrt{\sigma_{i+1}^2 - \sigma_i^2}$, and $\sigma_0 = 0$ we recover exactly the distributions $u_i \sim p_{\sigma_i}(u_i)$ previously introduced in the context of denoising score matching. This choice is referred to as *variance-exploding* (VE) diffusion. Another popular choice is to pick $\beta_i \in (0, 1)$ and $\alpha_i = \sqrt{1 - \beta_i^2}$ such that the variance $\mathbb{V}[u_i] = 1$ for all i if $\mathbb{V}[u_0] = 1$. Naturally, this approach is referred to as *variance-preserving* (VP).

As shown in [177] the Markov chain (26) admits a time-continuous formulation as a stochastic differential equation (SDE) of the form

$$(27) \quad du_t = f(t)dt + g(t)dB_t, \quad 0 \leq t \leq T$$

with the initial condition $u_0 \sim p(u)$. Here B_t denotes Brownian motion. We denote the distribution at time t as $u_t \sim p_t(u)$. As $L \rightarrow \infty$ in (26) the VE diffusion scheme leads to the time-continuous formulation [177, Appendix B]

$$(28) \quad f(t) \equiv 0, \quad g(t) = \sqrt{\frac{d\sigma^2(t)}{dt}}$$

with an increasing function $\sigma(t)$ such that the final distribution satisfies $p_T(u) \approx \mathcal{N}(0, \sigma(T)^2 \mathbf{I})$. The VP diffusion scheme, on the other hand, results in

$$(29) \quad f(t) = -\frac{\beta(t)}{2}, \quad g(t) = \sqrt{\beta(t)}$$

and $p_T(u) \approx \mathcal{N}(0, \mathbf{I})$. Recall that our goal eventually is to revert the process (27). To do so we make use of a result shown in [10] stating that the SDE (27) admits a *reverse SDE*, that is, an SDE which flows backwards in time and leads to a process of the same distribution as (27). The reverse SDE reads as

$$(30) \quad du_t = [f(t) - g(t)^2 \nabla \log p_t(u)] dt + g(t) d\bar{B}_t$$

where now dt is a negative infinitesimal time step and \bar{B}_t denotes Brownian motion moving backwards in time.

A natural way of sampling from $p(u)$ using this framework is to discretize and simulate (30) from $t = T$ to $t = 0$ starting from the tractable distribution $p_T(u)$ [177, 176, 93]. In order to do so, in a training stage we first have to estimate the score $\nabla \log p_t(u)$ which is possible using denoising score matching (24).

Interestingly, it is also feasible to pursue a slightly different modeling approach which, however, turns out equivalent in the end. Note that (30) shows that the reverse diffusion is of the same functional form as the forward one. Thus, if $p(u_{i+1}|u_i) = \mathcal{N}(u_{i+1}; \alpha_i u_i, \beta_i^2 I)$ denotes the transition probabilities of the forward diffusion according to (26), the transition probabilities of the reverse diffusion, denoted as $q(u_i|u_{i+1})$, will also be Gaussian $q(u_i|u_{i+1}) = \mathcal{N}(u_i; \mu(u_{i+1}, i+1), \Sigma(u_{i+1}, i+1))$ where $\mu(u_{i+1}, i+1), \Sigma(u_{i+1}, i+1)$ are functions of the state u_{i+1} and the time step $i+1$. In practice the variance might be assumed to be fixed fixed, e.g., as $\Sigma(u_{i+1}, i+1) = \beta_{i+1}$ [93]. Thus, instead of training the score, we can instead as well train the means of the reverse diffusion $\mu_\theta(u_{i+1}, i+1) \approx \mu(u_{i+1}, i+1)$ using a neural network μ_θ . To be precise, the approximations $\mu_\theta(u_{i+1}, i+1)$ lead to transition probabilities $q_\theta(u_i|u_{i+1})$ and eventually to the distribution $q_\theta(u_0)$ which we can use for maximum likelihood estimation, that is, maximizing $\theta \mapsto \mathbb{E}_{u \sim p(u)} [\log q_\theta(u_0)]$ so that $q_\theta(u_0) \approx p(u)$. A lower bound $L(\theta)$ for this objective is derived in [173, 126] as

$$(31) \quad L(\theta) = \sum_{i>1} \mathbb{E}_{u_0 \sim p(u)} [\text{KL}(p(u_{i-1}|u_i, u_0) \| q_\theta(u_{i-1}|u_i))] + \text{const.}$$

It turns out that, in the case of Gaussian transitions $p(u_{i+1}|u_i)$, training via (31) is, indeed, equivalent to training a score $s_\theta(u_i, i) \approx \nabla \log p_{t_i}(u_i)$ via denoising score matching. The approximated score can be used to compute the means $\mu_\theta(u_{i+1}, i+1)$ of the reverse diffusion transition probabilities and vice versa [93, 126].

An interesting work worth mentioning in this context is also [208], where the authors do not approximate the unknown density $p_t(u)$ using a general neural network, but show analytically that certain Gaussian mixture models solve the diffusion process exactly. The remaining parameters of these models are then trained using denoising score matching.

Having access to the trained score $s_\theta(u_i, i) \approx \nabla \log p_{t_i}(u_i)$, some authors propose to complement the approximation of the reverse diffusion with iterations of a MCMC sampling method for the distribution $p_{t_i}(u_i)$ for fixed t_i . Thus, the output of one step of the reverse diffusion process acts as a proposal which is then used as initialization for multiple steps of an MCMC method. This technique of alternating (reverse) time steps with MCMC steps for fixed time is referred to as *predictor/corrector sampling* [49, 177]. To reiterate, altogether three prevalent sampling methods appear within the realm of diffusion based methods: 1) Annealed Langevin sampling [174], i.e., MCMC sampling from successively less noisy distributions, 2) purely discretizing the reverse SDE [177, 176, 93], and 3) as a mixture of the two predictor/corrector sampling [49, 177]

Application to inverse problems: By now, we have explained how score-based and diffusion models are used to approximately sample from a complex distribution $p(u)$. In view of inverse problems we are, however, interested in samples from $p(u|y)$ where y denotes the

given observation. Various techniques to incorporate the observation have been proposed in the literature.

In [49, 69] the authors apply a diffusion model to MRI and incorporate the observation by performing predictor/corrector sampling for $p(u)$ and gradient descent steps for the data fidelity in an alternating fashion. In [176] a stochastic process $y_t = A u_t + \zeta$ for the observation corresponding to u_t is defined and for sampling the authors alternate steps of a discretization of the reverse diffusion with proximal data consistency steps, which balance data consistency to y_t and deviations from the previous iterate. Also in [48] the strategy of alternating reverse diffusion steps with data consistency steps is employed. The authors additionally propose to initialize the reverse diffusion with the output of the forward diffusion process starting from an initial guess of the solution which can be computed efficiently. This process acts as an acceleration.

In [126, 173] the authors derive expressions for the transition probabilities conditioned on the observation $q_\theta(u_{i-1}|u_i, y)$ using Bayes theorem. Similarly, in [177], the authors derive an approximation for the conditional score $\nabla \log q_\theta(u_t|y)$ given an observation for the inverse problem.

In [46, 47] the conditional score is factorized as $\nabla_{u_t} \log p(u_t|y) = \nabla \log p(y|u_t) + \nabla_{u_t} \log p(u_t)$. The latter is estimated using score matching whereas the former is approximated by $\nabla_{u_t} \log p(y|\hat{u}_0)$ with $\hat{u}_0 = \mathbb{E}[u_0|u_t]$ using Tweedie's formula [66]. Sampling can then be performed by approximating the reverse diffusion process with the techniques explained above. In [45] this approach is extended to blind inverse problems where the forward operator depends on unknown parameters as well.

In [108], the authors consider an approach inspired by denoising score matching [174]. However, they carefully design the noise additions in a way allowing for an explicit computation of the conditional score $\log p_\sigma(\tilde{u}|y)$ given the unconditional one $\log p_\sigma(\tilde{u})$ for which they utilize a SVD of the forward operator.

In [107] the forward and the backward diffusion are defined conditioned on the observation. However, training such a model is undesirable as it depends on the observation y . The authors provide a remedy by presenting a result stating that the training of the conditional model is equivalent to that of the unconditional one if there is no weight sharing of networks at different time steps.

3.3. Plug and Play Priors. Recall that MAP estimation is performed by solving

$$(32) \quad \arg \min_u \mathcal{D}_y(A u) + \lambda \mathcal{R}(u)$$

with the interpretation $p(y|u) \propto \exp(-\mathcal{D}_y(A u))$ and $p(u) \propto \exp(-\lambda \mathcal{R}(u))$. Different methods for solving (32) numerically have been proposed in the literature, such as proximal-gradient (forward-backward) methods [40, 34, 53]

$$(33) \quad u^{k+1} = \text{prox}_{\tau\lambda\mathcal{R}} \left(u^k - \tau\lambda A^* \nabla \mathcal{D}_y(A u^k) \right)$$

and its accelerations [27], ADMM optimization [31, 190]

$$(34) \quad \begin{cases} u^{k+1} = \text{prox}_{\frac{1}{\mu}} D_y \circ A (v^k - w^k) \\ v^{k+1} = \text{prox}_{\frac{\lambda}{\mu}} \mathcal{R} (u^{k+1} + w^k) \\ w^{k+1} = w^k + u^{k+1} - v^{k+1} \end{cases}$$

or primal-dual methods [38]

$$(35) \quad \begin{cases} v^{k+1} = \text{prox}_{\sigma \mathcal{D}_y^*} (v^k + \sigma A \bar{u}^k) \\ u^{k+1} = \text{prox}_{\tau \lambda \mathcal{R}} (u^k - \tau A^* v^{n+1}) \\ \bar{u}^{n+1} = 2u^{k+1} - u^k. \end{cases}$$

Similar to the derivation of score-based models, we can observe that non of these methods utilizes the mapping \mathcal{R} explicitly, however, they all at some point make use of the proximal mapping

$$(36) \quad \text{prox}_{\lambda \mathcal{R}}(u) := \arg \min_v \frac{1}{2} \|u - v\|_2^2 + \lambda \mathcal{R}(v).$$

Note, however, that $\text{prox}_{\lambda \mathcal{R}}(u)$ is simply the MAP estimate with respect to the observation u in the case of Gaussian noise and with the prior $p(u) \propto \exp(-\lambda \mathcal{R}(u))$. Consequently, in [190] it is proposed to replace $\text{prox}_{\lambda \mathcal{R}}(u)$ with a pre-trained denoiser $D(u)$ mapping noisy to clean images which is referred to as *plug and play* (PnP). This idea of [190] motivated a large body of follow up works employing different variations of PnP. In [190, 35] the PnP approach was based upon the iterations of ADMM. Subsequent works made use of other convex optimization approaches as mentioned, such as FISTA [104], half-quadratic splitting [213, 211], or proximal-gradient iterations [160]. Interestingly, in [130] it is shown that the fixed points of PnP derived from proximal-gradient iterations, ADMM, or primal-dual iterations are, in fact, identical.

In [186] the authors consider the variational problem

$$(37) \quad \min_{u, \tilde{v}} \lambda \|\tilde{v} - u\|_2^2 + \mathcal{R}(u), \quad \text{s.t. } A \tilde{v} = y$$

for which - inspired by PnP - the proximal step is replaced by a denoiser.

A lot of the subsequent works proposed to use CNN based denoisers within PnP approaches. For instance, in [213, 211, 160, 186, 130] the authors use CNNs trained for end-to-end denoising either directly or in a residual way such that the CNN reconstructs the noise. A specifically delicate training procedure involving adversarial training of the denoiser is employed in [151]. In [182], on the other hand, the trainable non-linear reaction diffusion (TNRD) denoiser from [43] is used. We want to emphasize at this point that the CNN denoisers used in the context of PnP methods are typically trained to remove noise using pairs of clean and noisy images rendering them as supervised methods conceptually. However, since in the context of PnP methods a pre-trained denoiser can be used for any inverse problem and does not rely on labeled training for the specific problem at hand, we still categorize them as unsupervised in our survey.

In [202, 59], on the contrary, the denoiser is trained on image pairs consisting of the noisy filtered back-projection and the ground truth data from CT imaging, rendering this approach fully supervised as also the specific forward model is incorporated in the labeled training data.

The empirical success of PnP methods was succeeded by theoretical considerations. Of course, it is easy to see that in the case that the denoiser is in fact the proximal mapping of some appropriate, convex functional \mathcal{R} , $D(u) = \text{prox}_{\mathcal{R}}(u)$, convergence of PnP schemes is a simple consequence of convergence of the corresponding convex optimization method (ADMM, proximal-gradient, etc.). This can be shown based on a classical result by Moreau [132], under the rather strong conditions that the denoiser has a symmetric Jacobian with eigenvalues in $[0, 1]$ [178].

In [39] convergence for ADMM PnP with an increasing penalty parameter within the ADMM scheme is shown assuming a bounded denoiser, in the sense that $\|D_{\sigma}(x) - x\|_2^2/n \leq c\sigma^2$ for all noise levels σ . In [182] ergodic convergence of ADMM PnP is proven if the denoiser is *averaged*, a property which can, e.g., be ensured by employing a specific network type referred to as *proximal neural networks* [85]. These are neural networks which consist of a concatenation of proximal mappings [85, Lemma 5.3]. In [160] convergence for proximal-gradient PnP and ADMM PnP is proven using fixed point arguments by enforcing Lipschitz continuity on the residual CNN denoiser.

3.3.1. Plug and Play via Tweedie. A slightly different approach to PnP which is closely related to the derivation of score based modeling in [174] is to approximate the true prior distribution $p(u)$ by a smoothed version thereof, $p_{\sigma}(\tilde{u}) = p(u) * \mathcal{N}(0, \sigma^2 I)(\tilde{u})$, that is, the convolution with a Gaussian kernel. Tweedie’s formula then [66] states that

$$(38) \quad \mathbb{E}[u|\tilde{u}] = \tilde{u} + \sigma^2 \nabla \log p_{\sigma}(\tilde{u}).$$

Thus, if the denoiser satisfies $D_{\sigma}(\tilde{u}) \approx \mathbb{E}[u|\tilde{u}]$, we might approximate $\nabla \mathcal{R}(u) = \nabla \log p_{\sigma}(\tilde{u})$ by

$$(39) \quad \nabla \log p_{\sigma}(\tilde{u}) \approx \frac{1}{\sigma^2} (D_{\sigma}(\tilde{u}) - \tilde{u})$$

and use this approximation within gradient based algorithms for variational inference, respectively MAP estimation [29, 13], or for sampling from the posterior $p_{\sigma}(\tilde{u}|y)$ and subsequent MMSE or variance estimation [118]. While this only provides a method for inference of a smooth approximation of the target distribution, the discrepancy between $p_{\sigma}(\tilde{u})$ and $p(u)$ can be made arbitrarily small for $\sigma \rightarrow 0$ [118]. Moreover, in [5, Theorem 1] it is shown, that also the discrepancy between $\frac{1}{\sigma^2} (D_{\sigma}(\tilde{u}) - \tilde{u})$ and the gradient $\nabla \log p(u)$ tends to zero as $\sigma \rightarrow 0$ if the denoiser is trained minimizing the squared error of the reconstruction for Gaussian noise corruption. In [76] such a PnP approach is used to simultaneously estimate the noise level and an MMSE reconstruction of the inverse problem.

3.4. Regularization by Denoising. In [153] the authors proposed *regularization by denoising* (RED), an approach sharing similarities with PnP priors. Specifically, the authors

introduce a RED regularizer defined as

$$(40) \quad \mathcal{R}(u) = u^T (u - D(u))$$

where $D(u)$ denotes a denoiser. The denoiser is assumed to satisfy two crucial conditions, namely, i) local homogeneity, that is, $D(cu) = cD(u)$ for $|1 - c| < \epsilon$ and ii) stability, i.e., the spectral radius satisfies $\max_i |\lambda_i(\nabla D(u))| < 1$ for all u where λ_i denote the eigenvalues of the Jacobian of the denoiser. These conditions are empirically demonstrated for several denoising methods (K-SVD [67, 127], BM3D [51], NLM [36, 109, 183], EPLL [216], and TNRD [43]) where it should be mentioned that differentiability is not given for EPLL, BM3D, and K-SVD as is.

In [153] the authors claim that, based on the assumptions, the RED regularizer satisfies $\nabla \mathcal{R}(u) = u - D(u)$ which is used in subsequent gradient based approaches for variational inference, such as gradient descent, ADMM, and a fixed point iteration for determining roots of the gradient of the objective functional, that is, u such that

$$(41) \quad 0 = \nabla_u (\mathcal{D}_y(Au) + \lambda \mathcal{R}(u)).$$

The approach is applied with two different denoisers D , a simple median filter and TNRD [43] as a CNN based method.

It was shown later, that the claims made in [153] are not always true. To be precise, for continuously differentiable denoisers the identity $\nabla \mathcal{R}(u) = u - D(u)$ is only satisfied in the case that the Jacobian of the denoiser $D(u)$ is symmetric [149]. Otherwise, there exists no regularizer admitting $u - D(u)$ as its gradient which is a direct consequence of Schwarz's theorem. In [149] it is also empirically verified, that the gradient identity $\nabla \mathcal{R}(u) = u - D(u)$ is significantly violated for the TNRD denoiser [43] and the CNN denoiser [212]. Despite these insights it is shown in [149] that for non-expansive denoisers, the RED fixed point iteration is, in fact, convergent (however, not to a minimizer of a variational regularization problem with a RED regularizer).

Further theoretical analysis was provided in [50] where the authors consider a slightly different approach. In this work the denoisers are assumed to be demicontractive and satisfy $D(0) = 0$. After showing that $D(u) = u$ is equivalent to $\mathcal{R}(u) = u^T (u - D(u)) = 0$ - that is, the fixed points of the denoiser coincide with the roots of the RED regularizer - the authors propose to solve

$$(42) \quad \min_u \mathcal{D}_y(u), \quad \text{s.t. } D(u) = u.$$

For this optimization problem a provably convergent hybrid steepest descent algorithm is presented. The method (as well as a relaxed version) is tested on several inverse problems with multiple denoisers, in particular, again TNRD [43].

In [95] RED is accelerated employing vector extrapolation. While empirically the method performs as expected, achieving the theoretically necessary conditions for convergence "might not be realistic in practice". The authors tested the method TNRD [43].

In [181] the RED approach is adapted to a block coordinate structure. Within the proposed gradient descent algorithm different coordinate blocks of u are updated separately chosen at random. The updates within the algorithm admit ergodic convergence to zero

in expectation if the denoiser is non-expansive for each coordinate block. In particular, under the stronger assumption that the denoiser is the proximal mapping of a function with bounded subgradient, the objective function value converges to its minimum in expectation. Experimental results are provided with an end-to-end CNN denoiser and other non-CNN based methods (TV and BM3D).

Similarly, in [196] the authors consider a stochastic gradient descent based algorithm for RED for which they show ergodic convergence to zero of the updates in expectation. In experiments they use a CNN denoiser trained to remove additive Gaussian noise.

An application of RED to phase retrieval using the residual CNN denoiser from [212] can be found in [131].

4. SUPERVISED

In this section we consider the case of having access to an iid sample $(u_i, y_i)_i$ of ground truth-observation pairs for training. The discussed supervised methods are classified into four categories: i) fully learned, ii) post-processing, iii) unrolling, and iv) learned regularizers. In i) the entire reconstruction $y \mapsto u$ is learned, whereas in ii) we use a trained method to improve upon a model based reconstruction. Methods according to iii) utilize NNs whose architecture resemble well-established iterative methods for solving inverse problems. That is, a layer of the NN might, e.g., share similarities to proximal-gradient iterations for (2). In iv) a regularizer is trained similarly as described in Section 3.2, however, this time training is performed in a supervised manner.

4.1. Fully Learned. The conceptually simplest approach to use neural networks for solving inverse problems might be what we refer to as *fully learned* in this article (cf. *direct Bayesian inversion* [17, Section 5.1.2]). This terminology refers to training a neural network \mathcal{N}_θ to directly map the observation y to a point estimate of u [215, 214]. The prototypical training problem for fully learned approaches reads as

$$(43) \quad \min_{\theta} \sum_{i=1}^N \ell(u_i, \mathcal{N}_\theta(y_i))$$

where $(u_i, y_i)_i$ denotes a given data set of ground truth/observation pairs satisfying $y_i = A u_i + \zeta_i$ with iid noise realizations ζ_i . Of course, Equation (43) can be modified to include, e.g., regularization of the parameters θ . In the case of fully supervised approaches, the trained method has to capture not only the prior distribution or the noise but also the forward model A . In particular, this means that for any different inverse problem the method has to be trained again, whereas unsupervised approaches can be used for different forward operators as long as the distribution $p(u)$ is unchanged. The potentially increased complexity due to implicitly learning the (reverse) forward operator, however, is not an issue in the case of image denoising, for which the forward operator reduces to the identity. Thus, denoising is particularly suited for fully learned approaches [101]. A lot of works in this context proposed to train residual neural networks. That is, instead of estimating the ground truth u , the network estimates the noise, respectively the residual, $\mathcal{N}_\theta(y) \approx y - u$ [77, 185, 212].

4.2. Post-processing. In the context of non-trivial forward operators, an approach significantly more popular than fully learned methods is data-driven post-processing. Instead of learning the entire mapping $y \mapsto u$, in this case, the neural network is preceded by a model-based reconstruction. That is, the neural network is trained to remove any remaining artifacts or noise that are still present after the non-learned reconstruction.

Substantial research has been conducted for post-processing of MRI [145, 198, 164, 96] and CT [102, 142, 41, 105] reconstructions where the zero filling solution and the result obtained via filtered backprojection (FBP), respectively, are further improved by a pre-trained NN.

While training of supervised methods is often performed by simply minimizing the reconstruction loss on a given data set [102, 142, 41], a lot of works on post-processing propose adversarial training. In this case, well-known GAN training, according to (12) or (16), has to be adapted to fit the post-processing task, e.g., the model parameters are obtained as solutions to

$$(44) \quad \min_{\theta} \max_{\phi} \mathbb{E}_{\tilde{u} \sim p(\tilde{u})} [\log(1 - D_{\phi}(G_{\theta}(\tilde{u})))] + \mathbb{E}_{u \sim p(u)} [\log(D_{\phi}(u))] \\ + \mathbb{E}_{(u, \tilde{u}) \sim p(u, \tilde{u})} [\ell(G_{\theta}(\tilde{u}), u)]$$

where \tilde{u} denotes the corrupted images obtained after applying the model based reconstruction to the observation y . The first two terms in (44) resemble the usual GAN loss. In the third term, $\ell(G_{\theta}(\tilde{u}), u)$ denotes some kind of discrepancy measure between the reconstruction obtain via post-processing and the actual ground truth. For instance, ℓ might be chosen as a simple MSE loss or a perceptual VGG loss [198]. Note that in this formulation the generator input is not a random sample from a pre-specified latent distribution, but the corrupted image data.

Several variations of GAN training for post-processing have been proposed. In [145] the authors combine the GAN loss with the MSE or MAE loss in the image as well as in the frequency domain for improving upon the zero filling reconstructions for MRI. In [198] additionally a perceptual VGG loss is included. In [199] a Wasserstein GAN is combined with a VGG loss for post-processing of low-dose CT images. A different approach is pursued in [205] where the authors propose to simultaneously train two GANs for post-processing of low resolution CT images. One of the generators maps from low to high resolution and the other one in the opposite direction. The authors employ a Wasserstein GAN loss complemented with additional functionals ensuring, in particular, that the two generators are, indeed, inverse functions of each other.

Another viable approach are conditional GANs [98] where the generator has two inputs, the corrupted data and a random sample $G_{\theta}(\tilde{u}, z)$. Thus, during application of the method, for fixed \tilde{u} sampling *conditioned on* \tilde{u} is possible by sampling from z .

4.3. Unrolling. *Unrolling* or *learned iterative methods* (first proposed in [73]) is a way of designing end-to-end networks for the solution of inverse problems in a more deliberate way. Let us consider the output u^L of a generic L layer feed-forward neural network according

to

$$(45) \quad u^{k+1} = \sigma \left(W_k u^k + b_k \right), \quad k = 0, 1, 2, \dots, L - 1$$

where $(W_k, b_k)_k$ are the weights and biases of the network, σ is the non-linearity, and u^0 is its input. Note that, if we choose the weights and biases as $W_k = (I - \tau\lambda A^* A)$, $b_k = \tau\lambda A^* y$ for all k , and the non-linearity as $\sigma(u) = \text{prox}_{\tau\lambda\mathcal{R}}(u)$, (45) matches exactly L iterations of the proximal gradient algorithm with step size τ

$$(46) \quad u^{k+1} = \text{prox}_{\tau\lambda\mathcal{R}} \left(u^k - \tau\lambda A^* (A u^k - y) \right)$$

for solving

$$(47) \quad \min_u \frac{1}{2} \|A u - y\|_2^2 + \lambda \mathcal{R}(u).$$

Thus, we find a close resemblance between the structure of neural networks and iterative methods for variational regularization. This observation is the foundation of unrolling: Instead of choosing an arbitrary network architecture for solving the inverse problem at hand in an end-to-end fashion, it seems more reasonable to make design choices (loosely) imitating iterations of an optimization method. Specifically, we might keep some parts of the iteration (46) and replace others by trainable building blocks, e.g., in [197] the authors train only the non-linearities. The training approach of unrolled methods is a crucial difference between unrolling and PnP (Section 3.3). While the two frameworks share similarities in the sense that in both cases one aims to replace certain parts of a well-established iterative method with trainable components, unrolled methods are considered end-to-end and trained in a supervised way according to (43). In PnP methods, on the other hand, the learned component is pre-trained in an unsupervised way and simply "plugged" into the iteration. As a consequence, as in general for supervised methods, the approach in unrolling renders training dependent on the forward operator A , such that the trained method cannot be applied to a different inverse problem in general.

The principle of unrolling outlined above is of course not restricted to proximal gradient iterations [73, 197, 193], which were used as an instructive example, but applicable to any optimization method such as gradient descent [3, 143, 83], ADMM [200, 201, 86], primal-dual algorithms [4] or, as in [43], to the discretization of a reaction-diffusion equation.

A typical modeling question in the context of unrolling is how much of the method is allowed to be trained and which parts are kept as in the underlying iterative method. In [197, 210] the gradient step of a proximal-gradient method is kept as is, whereas the proximal mapping is replaced by a trained version. A similar and empirically successful approach is pursued in the learned primal-dual algorithm [4], where the authors replace the proximal mappings of a primal-dual method by trained CNNs. They additionally improve numerical performance by introducing memory to the algorithm, that is, information of previous iterates is included when computing the next update. In [193] on the contrary, the authors unroll a proximal gradient method and preserve the proximal steps, whereas they allow for trainable gradient updates.

Another related modeling question is whether to employ *weight sharing*. Weight sharing refers to imposing an additional constraint on the unrolled network ensuring that the weights/non-linearities of different layers are identical [193, 197]. This technique reduces the number of trainable parameters and is clearly reasonable if the update rule of the underlying iterative method is identical in each iteration as, e.g., in (46). An interesting insight in this context is that weight sharing is closely related to recurrent neural networks as having consecutive layers with identical weights might as well be modeled as a single layer with a feedback loop [143]. On the other hand, increasing flexibility by allowing different weights at different layers might lead to improved performance [4, 210, 43, 83] at the cost of higher complexity and less interpretability.

4.4. Learned Priors. In addition to the above approaches where an image-to-image mapping is learned, there are several approaches for training a regularization functional, respectively prior, $\mathcal{N}_\theta(u) = \mathcal{R}(u)$ in a supervised way (contrary to the unsupervised approaches in Section 3.2). A rather intuitive formulation to achieve this is a bilevel optimization scheme aiming to minimize the reconstruction error [116, 54], e.g.,

$$(48) \quad \begin{cases} \min_{\theta} \sum_{i=1}^N \|\hat{u}_i(\theta) - u_i\|_2^2 \\ \text{s.t. } \hat{u}_i(\theta) = \arg \min_u \mathcal{D}_{y_i}(A u) + \mathcal{R}_\theta(u). \end{cases}$$

Closely related, in [113, 114], the authors propose total deep variation regularization. They model the regularizer as $\mathcal{R}(u) = \sum_{i,j} \mathcal{N}_\theta(u)_{i,j}$ where \mathcal{N}_θ is a U-net style network of a certain structure and the sum is taken over all output pixels of the network. In [113, 114] the solution of the variational regularization problem is formulated as a gradient flow instead of an iterative gradient descent scheme, which allows to phrase the training problem as an optimal control problem. In a discretized setting, however, this leads to a formulation similar to (48). The authors of [113, 114] include proofs for existence of solutions of the training problem as well as a stability analysis.

A different approach for training is pursued in [125, 134]. There the authors propose an adversarial training strategy according to

$$(49) \quad \min_{\theta} \mathbb{E}_{u \sim p(u)} [\mathcal{N}_\theta(u)] - \mathbb{E}_{y \sim p(y)} [\mathcal{N}_\theta(A^\dagger y)] + \mathbb{E}_{\hat{u} \sim p(\hat{u})} [(\nabla \mathcal{N}_\theta(\hat{u}) - 1)_+^2]$$

where A^\dagger denotes the (possibly regularized) pseudo-inverse of A and $p(\hat{u})$ denotes a uniform distribution on straight lines between a sample from $p(u)$ and a sample $A^\dagger y$ for $y \sim p(y)$ (cf. Section 3.1.4). The first two terms ensure that the regularizer yields small values on true samples from $p(u)$ and large values on plain pseudo-inverse reconstructions. The third term, on the other hand, enforces Lipschitz-1 continuity of \mathcal{N}_θ which relates the training problem to the Wasserstein-1 distance [125].

Another different training strategy is pursued in [120, 12]. Given a data set $(u_i)_i$ of ground truth images, a neural network \mathcal{N}_θ is trained to map $\mathcal{N}_\theta(u_i) \approx 0$ for some i and $\mathcal{N}_\theta(A^\dagger A u_i) \approx A^\dagger A u_i - u_i$ for the remaining samples. That is, the network maps ground truth images to zero and reconstructions obtained via the pseudo inverse to their residuals

to the ground truth. In [120] the network \mathcal{N}_θ is designed as an auto-encoder $\mathcal{N}_\theta = D_{\theta_2} \circ E_{\theta_1}$ and as a regularizer the authors use the norm of the latent variable $\mathcal{R}(u) = \|E_{\theta_1}(u)\|_q^q$. In [12] the regularizer is directly chosen as $\mathcal{R}(u) = \|\mathcal{N}_\theta(u)\|_2^2$.

5. UNTRAINED MODELS

In contrast to supervised and unsupervised methods, where the training of models using training data is an essential building block, untrained neural-network based approaches do not require training, but rather rely on the architecture of the neural network itself to act as a prior for image data. In this section, we summarize some of the main techniques used in this context. For further information we refer to the review paper [144], which focuses exclusively on untrained neural network priors.

The research field of untrained neural network approaches for inverse problems in imaging was initiated by [188]. The main idea of such approaches is to constrain the unknown image data to be in the range of a neural network, whose parameters are optimized to fit the measurement data. This results in approaches of the form

$$(50) \quad \min_{u, \theta, z} \mathcal{D}_y(Au) \quad \text{s.t. } u = \mathcal{N}_\theta(z),$$

which can equivalently be written as

$$\min_{\theta, z} \mathcal{D}_y(A\mathcal{N}_\theta(z)).$$

While the baseline approach above optimizes over both the latent variable z and the network parameters θ , in the original work [188] the latent variable z is fixed and initialized with uniform noise between 0 and 0.1 as default. The network \mathcal{N}_θ used in [188] has a fully convolutional architecture of U-net-type [155], with the input and output dimensions being equal. The default network architecture uses skip connections, LeakyReLU as activation function, strides for downsampling and bilinear interpolation for upsampling.

The network used in [188] is highly overparametrized (the default architecture has around two million parameters), such that in practice it is capable of fitting also noisy data. However, the authors of [188] argue that, following the trajectory of a gradient decent algorithm to minimize the objective (50), clean images are approximated first and noise or image artifacts appear only in later iterations. Consequently, early stopping is used to achieve a regularization effect.

A second influential work in the context of untrained approaches uses a different strategy to avoid the approximation of noise: The deep decoder network of [88] uses a simple, non-convolutional architecture with less weight parameters than degrees of freedom in the output. Specifically, for a tensor $z_i \in \mathbb{R}^{n_i \times k_i}$, the tensor $z_{i+1} \in \mathbb{R}^{n_{i+1} \times k_{i+1}}$ of the $(i+1)$ layer for $i = 0, \dots, L-1$ is obtained as

$$z_{i+1} = \text{cnReLU}(U_i z_i W_i),$$

where $W_i \in \mathbb{R}^{k_i \times k_{i+1}}$ are the weights, $U_i \in \mathbb{R}^{n_{i+1} \times n_i}$ is an upsampling matrix realizing bilinear upsampling (and the identity in case of U_{L-1}) and cn performs a pointwise normalization of each channel. The final output of the network is then computed as

$$u = \text{sigmoid}(z_L W_L).$$

Note that by using the matrix multiplication $z_i W_i$ as weighted connection between consecutive layers, the deep decoder differs significantly from a fully connected neural network in that, for a fixed input and output channel, the same weight is used for all spatial positions. This corresponds to what is often referred to as 1×1 convolution, and in the continuous setting corresponds to a convolution with a weighted delta peak at 0.

Default network dimension used in [88] are $L = 6$, $n_0 = 16 \times 16$, $n_d = 512 \times 512$ and $k_i = k = 64$ or $k_i = k = 128$. Like in [188], the input variable $z = z_0$ is chosen randomly and fixed.

The main difference of this model to the original deep image prior of [188] is that, due to underparametrization, the deep decoder cannot fit arbitrary data such that no regularization by early stopping is required. This is argued by the authors of [88] by providing in [88, Proposition 1] a lower bound (that holds with high probability) of how well a single layer deep decoder can approximate zero mean Gaussian noise.

Again aiming to avoid the approximation of noise, a third class of untrained, neural network based approaches is considered in [78], where also an analysis in the infinite dimensional setting is carried out. There, a variational approach of the form

$$(51) \quad \min_{u,v} \mathcal{D}_y(Au) + \lambda_1 \mathcal{R}(u - v) + \lambda_2 \mathcal{G}(v)$$

is introduced, where (as special case of the more general framework analyzed in [78])

$$(52) \quad \mathcal{G}(v) = \inf_{\theta, (z_i)_{i=1}^L} \sum_{i=1}^L \|z_i\|_{\mathcal{M}} \quad \text{s.t.} \quad \begin{cases} v = \mathcal{N}_{\theta_1} \circ \dots \circ \mathcal{N}_{\theta_L}(z_L), \\ z_{i-1} = \mathcal{N}_{\theta_i}(z_i) \text{ for } i = 2, \dots, L, \\ \|\theta\|_2 \leq 1, M\theta = 0. \end{cases}$$

Here, $\mathcal{N}_{\theta_1} \circ \dots \circ \mathcal{N}_{\theta_L}$ maps the latent variable z_L to image data, and the \mathcal{N}_{θ_i} are convolutional layers mapping latent variables z_i (modeled as Radon measures) via a convolution with filters θ_i (modeled as L^2 functions) to latent variables z_{i-1} . Different to the previous two approaches, the layers \mathcal{N}_{θ_i} do not include nonlinearities directly, but a non-linearity is included indirectly via penalizing the Radon norm $\|\cdot\|_{\mathcal{M}}$ of the latent variables z_i , also at intermediate layers. In addition, for regularization, the weights $\theta_1, \dots, \theta_L$ are constrained in their L^2 norm, and an optional linear constraint (such as having zero mean) is included in the model.

Another particularity of this approach is that the neural network-type prior \mathcal{G} is employed via the infimal-convolution with a second regularization functional \mathcal{R} . This yields an energy-optimal, additive decomposition of the unknown as $u = (u - v) + v$, where $(u - v)$ is regularized via \mathcal{R} and v is regularized via \mathcal{G} . The reason for this extension is that, as argued in [78], neural-network priors are useful to generate highly structured, texture-like images, while for piecewise smooth images, classical priors such as the total variation [159]

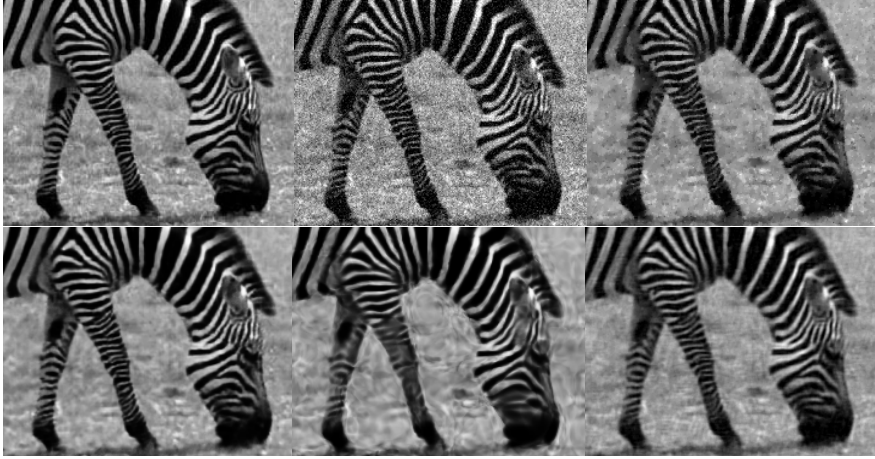


FIGURE 3. Results for denoising with additive Gaussian noise with zero mean and standard deviation 0.1 times the image range. First row: Original, corrupted, and TGV reconstruction [33]. Second row: Deep image prior [188], deep decoder [88], and the method from [78].

or higher-order extensions [33, 32] are already very well suited. This argument is supported in [78, 79] also by the analytic result that generator-networks such as (52) can, in the infinite resolution limit, only generate continuous functions as images, making it necessary to combine such priors with other approaches via infimal convolution in order to obtain a regularization that matches the established model of images having sharp edges in the form of jump discontinuities.

Besides numerical experiments, [78] also provides a function-space analysis of the approach (51), showing in particular well-posedness, a consistency result and the above-mentioned result on regularity of solutions. For an exemplary comparison of the deep image prior, the deep decoder and the approach (51) for denoising we refer to Figure 3.

Before moving to a discussion of works on the analysis and extension of deep-image-prior-based approaches for imaging, we also mention that such techniques have also been applied to dynamic data. See for instance [204, 52] for the application of the deep image prior to dynamic MRI or [2] for the application of an untrained neural-network based approach to the isolation of different types of motion in MRI.

5.1. Regularization Properties of Untrained Neural Networks. The, at first glance surprising, capability of the deep image prior to have a regularizing effect in image reconstruction has triggered many works that further analyze and aim to explain this capability.

The work [89] analyzes the denoising capabilities of gradient descent with early stopping to fit the deep decoder of [88] to noisy signals. Analytically this is done for a single-layer variant and under the assumption that the ground truth signal is in the span of p trigonometric basis functions, in which case an upper bound (that holds with high probability) on the difference between the denoised and the ground-truth signal is obtained that is of the

order $\sigma\sqrt{p/n}$, with σ^2 the variance of the noise and n the dimension of the signal. In a follow up work [90], it is further shown for compressed sensing problems with a Gaussian measurement matrix A that the limit of gradient descent for

$$\min_w \frac{1}{2} \|A \mathcal{N}(w) - A u^*\|_2^2,$$

where $\mathcal{N}(w)$ is again the output of a single-layer variant of the deep decoder, approximates u^* with high probability.

A conclusion drawn in [89] is that denoising capabilities of untrained models are primarily attributed to convolutions that use fixed, non-trainable interpolation kernels. Those are usually included in networks via upsampling operators. A similar conclusion is also made in [123], which considers spectral effects of upsampling and provides experimental results to conclude that upsampling is key to the denoising effects of untrained models (and, from that, also derives strategies for identifying suitable architectures for the deep image prior).

A different approach that allows to draw conclusions in particular on the regularization properties of untrained models is pursued in [79], which was already mentioned above. Here, the authors analyze the regularity of images generated by neural networks. Specifically, they introduce neural networks as mappings between function spaces and show that image-representing functions generated by CNNs with at least two layers are always continuous, and even continuously differentiable if the network input (i.e., the latent variable of the deepest layer) is of bounded variation. A connection to discretized CNNs mapping to images on pixel grids is made via Γ -convergence, showing that the discretized networks and energies used for training converge to the infinite resolution limit in an appropriate sense. A specific ingredient for the regularity result of [79] is that the convolution kernels are L^2 functions. In the context of network training or fitting an untrained network to data, this is implied by L^2 regularization of the network weights. Hence, a conclusion that can be drawn from [79] is that L^2 regularization of network weights in the deep image prior approach implies regularity of the resulting, network-generated image and thus avoids the approximation of noise, but on the other hand, hinders the reconstruction of sharp edges in the form of jump discontinuities.

Different to the above approaches, the works [58, 15] consider methods related to the deep image prior from a regularization-theoretic perspective. Specifically, they consider the minimization problem

$$(53) \quad \min_B \frac{1}{2} \|A u(B) - y\|_2^2 \quad \text{s.t.} \quad u(B) = \arg \min_u \frac{1}{2} \|Bu - y\|_2^2 + \lambda \mathcal{R}(u),$$

with B a linear operator and \mathcal{R} a regularization functional, and the solution $u(B)$ as surrogate for $\mathcal{N}_\theta(z)$ in the deep image prior objective (50). This different formulation is motivated by the fact that, in case \mathcal{R} admits a proximal mapping, the iteration

$$u^{k+1} = \text{prox}_{\tau\lambda\mathcal{R}}(u^k - \tau B^*(Bu^k - y)),$$

which converges to $u(B)$, resembles, for L steps, the forward pass of a neural network with particular architecture (cf. Section 4.3). The authors of [58] show that, in case $\mathcal{R} = \frac{1}{2}\|\cdot\|_2^2$ and B is constrained to have the same singular vectors as A , the mapping $y \mapsto u(B)$,

indeed, corresponds to a regularization method that carries out a filtering of the singular values of the forward map to approximate its pseudo inverse in a way lying in between well established truncated SVD and Tikhonov regularization. The work [15] further analyzes problems of the form (53) and shows in particular that, again if $\mathcal{R} = \frac{1}{2}\|\cdot\|_2^2$, they are in fact equivalent to classical Ivanov regularization [99].

5.2. Exact Recovery of Untrained Network Approaches in Compressed Sensing. A question very much related to regularization properties of untrained neural-network based approaches is the one of exact recovery capabilities of such approaches in a compressed sensing context.

An early work here is [189], which essentially shows that gradient descent with respect to the network weights θ on

$$\min_{\theta} \|y - A\mathcal{N}_{\theta}(z)\|_2^2$$

can fit any signal y arbitrarily close, and regards this as evidence that indeed early stopping or additional regularization is required for untrained models. More specifically, this result of [189] is shown for a single-layer network of the form $z \mapsto \mathcal{N}_{\theta}(z) = V \cdot \text{ReLU}(Wz)$ with $\theta = W$ being the unknown parameters and V being a fixed random matrix, and for an orthonormal measurement matrix A and the width of the hidden layer being sufficiently large. In order to avoid overfitting of noisy data, [189] further proposes to use additional TV regularization of the network output and Gaussian-prior-based regularization on the network weights, and also introduces a scheme to learn the parameters of these regularization functionals from data.

In [87], building on results of [30], it is shown that, if A is a random Gaussian matrix with sufficiently many measurements, $y = Au + \zeta$, and if $\hat{\theta}$ minimizes $\theta \mapsto \|y - A\mathcal{N}_{\theta}(z)\|_2$ up to an additive ϵ of the optimum with z fixed, then, with high probability,

$$\|u - \mathcal{N}_{\hat{\theta}}(z)\|_2 \leq 6 \min_{\theta} \|u - \mathcal{N}_{\theta}(z)\|_2 + 3\|\zeta\|_2 + 2\epsilon + 2\delta,$$

where δ is a parameter inversely proportional to the number of measurements.

Another work in this context is [100], which proves exact recovery results for linear inverse problems and compressive phase retrieval. Specifically, [100] introduces algorithms for these two problems that essentially alternate between a gradient step towards data fidelity and a projection to the range of a deep network, and show that the iterates converge to the ground truth in both cases. Main assumptions to achieve this are that the ground truth lies in the range of a generator network, that the sampling matrix obeys a (generalized) restricted isometry property and, in the case of phase retrieval, that the network weights are initialized appropriately and the number of measurements is sufficiently large.

In a more recent work [37] the gradient flow

$$(54) \quad \begin{cases} \dot{\theta}(t) = -\nabla_{\theta} \mathcal{D}_y(A(\mathcal{N}_{\theta}(z))) \\ \theta(0) = \theta_0 \end{cases}$$

is considered as surrogate for first-order decent algorithms applied to the deep image prior. Besides well-posedness, main results of [37] are that the state $\theta(t)$ converges to θ_{∞} being a

global minimizer of $\theta \mapsto \mathcal{D}_y(A(\mathcal{N}_\theta(z)))$ and, under a restricted injectivity condition, the explicit estimate

$$\|\mathcal{N}_{\theta(t)}(z) - u\|_2 \leq a(t) + b + c,$$

where u is the true solution such that $y = A(u) + \zeta$ and A is the (potentially non-linear) forward model. Here, $a(t)$ reflects the distance of the current state $\mathcal{N}_{\theta(t)}(z)$ to its limit u_∞ (and converges to zero for $t \rightarrow \infty$), b quantifies how close the range of the generator is to the true solution u , and c quantifies the level of the noise ϵ . In the linear case, the main assumption for the later result is a restricted injectivity condition on the forward model, which corresponds to the so called minimum conic singular value of A being positive. Using this, a connection to compressed sensing results like [100] is drawn in [37] by showing that, for certain sub-Gaussian measurement matrices, the minimum conic singular value is positive with high probability depending on the number of measurements.

5.3. Combining Untrained Approaches with other Regularization Functionals.

Based on the works discussed in the previous two subsections, there is a general agreement that overparametrized, untrained neural network approaches such as the deep image prior require some kind of regularization technique to avoid overfitting. While some of the previously discussed works already draw conclusions about suitable regularization strategies as consequence of their results, we now discuss works that explicitly focus on the combination of untrained models with additional regularization functionals.

The work [44], for instance, considers a Bayesian perspective on the deep image prior and uses ℓ^2 regularization as prior for the network weights and the input. Exploiting the Bayesian perspective, [44] further computes the MMSE (instead of the MAP) of posterior

$$(\theta, z) \mapsto \|y - \mathcal{N}_\theta(z)\|_2^2 + \|(\theta, z)\|_2^2$$

for inference. Results of [44] indicate that this avoids overfitting and thus the need for early stopping.

A different strategy, pursued for instance in [122], is to add TV regularization on the network output to avoid the approximation of noise, that is, to solve

$$\min_{\theta} \|y - \mathcal{N}_\theta(z)\|_2^2 + \lambda \text{TV}(\mathcal{N}_\theta(z))$$

instead of (50). Instead of a classical regularization functional like TV, an alternative approach is also to combine the DIP with a trained regularization functional. A popular example in this direction is the combination with regularization by denoising (RED) (cf. Section 3.4) as proposed in [128]. Here, the minimization problem is given as

$$\min_{(\theta, u, z)} \|y - A\mathcal{N}_\theta(z)\|_2^2 + \lambda u^T(u - D(u)) \quad \text{s.t. } u = \mathcal{N}_\theta(z),$$

where D can be any pre-trained denoiser. An advantage of this method (and the original RED approach) is that, by using specific algorithmic reformulation, approximate solutions to the above optimization problem can be computed without differentiating the learned denoiser.

6. FUNCTION SPACE ANALYSIS OF NEURAL-NETWORK-BASED APPROACHES

Classical regularization theory for inverse problems usually considers an infinite dimensional function space setting [68]. Beyond the independence of particular discretization schemes, reasons for the latter are that crucial concepts of regularization theory for inverse problems, such as ill-posedness of the forward map or the regularity of solutions, are much clearer defined in function spaces. This is in particular also true for inverse problems in imaging, where for instance the space of functions of bounded variation [9] provides a rich theory for regularity of image-representing functions, and spaces of measures are the natural setting for grid-independent sparse reconstruction problems.

In the context of neural-network-based approaches for inverse problems in imaging, function space analysis is still a niche topic, which has, however, grown in the past few years. While there exist already many works that analyze neural networks as mappings between function spaces, see for instance [42, 24, 115, 117, 79] or [81] for a recent, comprehensive review on infinite dimensional generative models, papers dealing specifically with the analysis of neural-network based approaches for inverse problems are still comparably rare. In this section, we strive to provide a brief overview of works in this context. In addition we refer to [135] for a review paper with an emphasis also on the analysis of neural-network based approaches for inverse problems.

An early work dealing with classical regularization theory for neural-network-based approaches to inverse problems is [166]. Here, the authors consider a specific type of neural network used for post-processing (see Section 4.2 for this type of approaches), for which they provide theoretical results. Given the forward model $A : \mathcal{X} \rightarrow \mathcal{Y}$ and any image-based neural-network $\mathcal{N}_\theta : \mathcal{X} \rightarrow \mathcal{X}$, [166] defines a deep null space network as $L = I_{\mathcal{X}} + P_{\ker(A)} \mathcal{N}_\theta : \mathcal{X} \rightarrow \mathcal{X}$ with $I_{\mathcal{X}}$ the identity operator on \mathcal{X} . This restricts the image-based regularization of the neural network to the kernel of A , such that $A L u = A u$. Combining this approach with any family $(B_\alpha)_\alpha$ of functionals comprising a regularization method, and assuming Lipschitz continuity of the network $\mathcal{N}_\theta : \mathcal{X} \rightarrow \mathcal{X}$, [166] shows that $(L \circ B_\alpha)$ also comprises a convergent regularization method. For further extensions and analysis of this approach we refer to [167].

Another, rather influential work providing function space results is [120]. Here the authors consider a regularizer of the form

$$\mathcal{R}(u) = \psi(\mathcal{N}_\theta(u)),$$

called NETT regularizer, where $\psi : \mathcal{X} \rightarrow [0, \infty]$ is a given, scalar valued functional and

$$\mathcal{N}_\theta(u) = (\sigma_L \circ \Theta_L \circ \dots \circ \sigma_1 \circ \Theta_1)(u),$$

with $\Theta_i : \mathcal{X}_{i-1} \rightarrow \mathcal{X}_{i-1/2}$ affine mappings (assumed to be parametrized by θ) and $\sigma_i : \mathcal{X}_{i-1/2} \rightarrow \mathcal{X}_i$ functions modeling the activation functions. Under assumptions such as weak continuity of the involved mappings and coercivity of \mathcal{R} , [120] obtains classical results of regularization theory, in particular well-posedness, convergence and convergence rates under source conditions.

The follow-up-work [138] aims to avoid the coercivity assumption of [120] by considering regularization functionals of the form

$$\mathcal{R}(u) = \psi(\mathcal{N}_\theta(u)) + \frac{c}{2} \|u - D_\theta \circ \mathcal{N}_\theta(u)\|_2^2,$$

where $\mathcal{N}_\theta : \mathcal{X} \rightarrow \ell^2$ and $D_\theta : \ell^2 \rightarrow \mathcal{X}$ are assumed to be encoder and decoder networks, respectively. Assuming weak sequential continuity in particular of the involved encoder and decoder network, [138] obtains again classical well-posedness and convergence results, where coercivity is now a consequence of the particular form of \mathcal{R} . The recent work [82] further extends this regularization approach to Morozov regularization.

A different, generator (or synthesis) based approach towards neural-network-based regularization in function space is considered in [139]. There, the authors consider a variational regularization approach of the form

$$\min_z \|A(\mathcal{N}_{\theta,\lambda}(z)) - y\|_2^2 + \lambda \|z\|_{1,w},$$

where $\mathcal{N}_{\theta,\lambda} : Z \rightarrow \mathcal{X}$ is a generator network (depending also on the regularization parameter λ) and $\|\cdot\|_{1,w}$ is a weighted ℓ^1 norm. Assuming the generator network $\mathcal{N}_{\theta,\lambda}$ to be weakly sequentially continuous, [139] obtains again well-posedness and convergence results for this approach.

Function space analysis for a related, generator-based regularization strategy was also considered in the aforementioned [78] via a variational approach of the form

$$(55) \quad \min_{u,v} \mathcal{D}_y(Au) + \lambda_1 \mathcal{R}(u-v) + \lambda_2 \mathcal{G}(v).$$

Recall that here, \mathcal{G} is a prior based on a generator network as defined in (52), and \mathcal{R} is an optional, classical regularization functional. Different to the approach of [139] above, [78] considers an untrained model in the spirit of the deep image prior [188]. Modeling latent spaces as Radon measures and filter kernels as L^2 functions, [78] proves weak-to-weak continuity of the involved, bilinear convolution operators and coercivity of the overall approach, from which well-posedness and convergence results follow using standard techniques. A particularity of [78] is that the explicit definition of convolutional neural networks as mapping between function spaces also allows to analyze regularity of solutions of (55). In particular, in [78] it is shown that the output of the generator network is always a continuous function, implying that solutions u, v of (55) satisfy $u = (u-v) + v \in \text{BV}(\Omega) + C(\Omega)$ in case \mathcal{R} is the total variation functional and $\Omega \subset \mathbb{R}^d$ is the domain of the image representing functions.

In this context, we also recall the work [79], which is already discussed in Section 5.1 and analyses the regularity of images generated by convolutional neural networks. In the context of regularization theory for neural network approaches in function space, it is also worth noting that, as supplementary result, [79, Theorem 3.15] provides well-posedness of the training of a large class of neural networks in function space by empirical risk minimization, without posing assumptions such as weak continuity or coercivity on the network.

An approach similar to the NETT regularizer of [120] is the adversarial regularization approach of [125] (see also Section 3.2). Here, the regularization functional is of the form

$$u \mapsto \mathcal{N}_\theta(u),$$

where \mathcal{N}_θ is a network trained to distinguish images coming from the true image distribution and images with artifacts being obtained via a direct reconstruction method. Besides well-posedness results under lower semi-continuity and coercivity assumptions, main results of [125] are that gradient descent on a perfectly trained regularizer moves images towards the ground truth image distribution, and that, if the training data lies on a manifold, a perfectly trained model projects to this manifold. An extension of [125] towards training input-convex adversarial regularizers is provided in [134], where input-convex neural networks in function spaces are defined as integral transforms with partially non-negative kernels to obtain convexity.

The work [6] analyses the learning of an optimal Tikhonov regularization approach in Hilbert spaces from a statistical perspective, where the unknowns u and the data $y = Au + \zeta$ are modeled as random variables in Hilbert spaces with joint distribution $p(u, y)$. Omitting - very interesting - technicalities from [6] that are necessary to rigorously define the statistical setup in a function space setting, the main idea is to solve

$$(56) \quad \min_{h, B} \mathbb{E}_{(u, y) \sim p(u, y)} \|R_{h, B}(y) - u\|_{\mathcal{X}}^2 \quad \text{where } R_{h, B}(y) = \arg \min_u \mathcal{D}_y(Au) + \|B^{-1}(u - h)\|_{\mathcal{X}}^2.$$

As shown in [6], $(h, B) = (\mu, \Sigma_x^{1/2})$, with μ and Σ_x the mean and covariance of the random variable describing the ground truth image distribution, is always a solution to (56), which is in particular independent of the forward model. These results are further extended in [6] to training with finitely many samples via convergence results.

Related to the previous work, in [103] the authors consider the learning of a filter function either for spectral regularization or for the filtered-backprojection for the Radon transform. In the former case, assuming the forward operator A to be compact and to be given via the singular value expansion as

$$Au = \sum_{n=1}^{\infty} \sigma_n \langle u, u_n \rangle v_n,$$

the spectral regularization approach takes the form

$$R(y^\delta, g_\delta) = \sum_{n=1}^{\infty} g_\delta(\sigma_n) \langle y^\delta, v_n \rangle u_n,$$

where g_δ is a learned function with $g_\delta(\sigma) \rightarrow 1/\sigma$ as $\delta \rightarrow 0$ and δ is the noise level. A result of [103] is that, in the ideal case of minimizing the true risk, the optimal filter function is given as

$$g(\sigma_n) = \frac{\sigma_n \Pi_n}{\sigma_n^2 \Pi_n + \Delta_n}$$

where $\Pi_n = \mathbb{E}_u(\langle u, u_n \rangle^2)$ and $\Delta_n = \mathbb{E}_\zeta(\langle \zeta, v_n \rangle^2)$, with ζ the additive measurement noise. Beyond that, [103] provides convergence results for the learned regularization.

The work [16] considers a residual network, i.e., networks of the form

$$\varphi_\theta(x) = x - \mathcal{N}_\theta(x)$$

to approximate the forward operator A , and then exploits inversion of φ_θ via a fixed point iteration to approximate A^{-1} . Following this approach, [16] provides well-posedness and convergence results, and also considers particular architectures of \mathcal{N}_θ and the relation to spectral regularization methods.

In a different context, [65] considers the analysis of PnP methods (see Section 3.3 for details) as regularization methods. Specifically, they consider iterations of the form

$$u_{n+1} = (\mathcal{N}_\theta(\lambda, \cdot) \circ (\text{I} - s\nabla_u \mathcal{D}_y))(u^n),$$

where $\mathcal{N}_\theta(\lambda, \cdot)$ is a learned denoiser depending on the regularization parameter λ . Assuming that $\mathcal{N}_\theta(\lambda, \cdot)$ is a contraction and that $\mathcal{N}_\theta(\lambda, \cdot)$ converges to the identity as $\lambda \rightarrow 0$ in an appropriate sense, [65] shows that the mapping of data to fixed points of the above regularization is a convergent regularization method.

The work [22] introduces data driven regularization via including a projection to training data. That this, given training pairs u_i and $y_i = A u_i$ for $i = 1, \dots, n$ as training data, [22] analyzes the regularization properties of the generalized inverse of $A P_{U_n}$, with P_{U_n} a projection to $U_n = \text{span}((u_i)_{i=1}^n)$, which is shown to be equal to

$$A^{-1} P_{Y_n}.$$

In [22] the explicit expression of $A^{-1} P_{Y_n}$ is further investigated in terms of orthonormal bases obtained from the training data, stability of the orthonormalization procedure and regularization properties of the overall resulting method. In particular, convergence in the case of noise free and noisy data is shown under appropriate conditions.

The paper [21] analyzes a data-driven Landweber iteration for non-linear inverse problems. The iteration is given as

$$u^{k+1} = u^k - A'(u^k)^*(A(u^k) - y) - \lambda_k B'(u^k)^*(B(u^k) - y),$$

where $B : \mathcal{X} \rightarrow \mathcal{Y}$ is a learned operator satisfying $B(u_i) = y_i$ for some training data $(u_i, y_i)_{i=1}^N$. The motivation for this data-driven adaption is that the damping term appearing in the classical Landweber iteration can be interpreted as a prior on the solution, and hence the penalization of $\|B(u) - y\|_2$ allows to include additional expert knowledge in the form of training data. Under appropriate assumptions, in particular the tangential cone condition, [21] obtains convergence results for the proposed modified Landweber iteration. Further results on convergence and stability of this method are also obtained in [23], and in the work [70] the method is further extended with a convex penalty term and acceleration techniques.

The work [163] analyzes a Gauss-Newton method in a setting conceptually related to sparse coding techniques and untrained models like the deep image prior. That is, [163] analyzes the Gauss-Newton method for solving

$$A \mathcal{N}_\theta(\cdot) = y$$

with respect to θ , where $\theta \mapsto \mathcal{N}_\theta$ maps finite dimensional parameters to a shallow neural network representing the unknown as function in L^2 . A result of [163] is in particular local quadratic convergence of the resulting method under appropriate conditions, in particular linear independence of activation functions and their derivatives.

Related to this is also the work [7], which considers pretrained deep generative models $\mathcal{N}_\theta : \mathbb{R}^S \rightarrow \mathcal{X}$ mapping from a finite dimensional latent space to image space. The work [7] rigorously introduces deep generative models mapping to function space via a wavelet-based multi-resolution analysis. It further investigates injectivity of the generator and provides a stability result for inverting non-linear forward models on the range space of the generator.

The work [26] further extends score based generative models to infinite dimensions (see also [81] for different approaches towards infinite dimensional generative models), and employs them to sample from a conditional distribution given the observed data in a Bayesian linear inverse problem setting.

7. QUANTIFYING UNCERTAINTY IN LEARNED MODELS

Uncertainty quantification is a central topic both in machine learning (see for instance [1] for a recent review) and inverse problems (see [184]). For the latter, recent works commonly adapt the Bayesian perspective on this topic [179], and we focus on this viewpoint also in this section.

The general approach in Bayesian uncertainty quantification is rather simple: As explained in Section 1, describing the data at hand as random variables (u, y) with a joint distribution $p(u, y)$, where typically $y = A(u) + \zeta$ with the random variable ζ describing measurement noise, Bayes' theorem provides the posterior distribution of u given an observation y as

$$p(u|y) = \frac{p(y|u) p(u)}{p(y)} \propto p(y|u) p(u).$$

Thus, in theory, given the data likelihood $p(y|u)$ and the prior $p(u)$, a full statistical description of the quantity of interest is available, from which point estimates (such as the MAP and MMSE) and information on uncertainty (such as variance or error quantiles) can be obtained. In practice, the situation is of course more difficult, and all main aspects of this approach comprise important research topics: Defining the data likelihood $p(y|u)$ is mostly a question of obtaining appropriate forward and noise models (and is often not in the focus of Bayesian approaches to inverse problems in imaging). Obtaining the prior $p(u)$ has received a lot of attention of the research community, where research has moved from hand-crafted priors to priors that are explicitly or implicitly learned from data, which was the main content of Section 3. Another vivid topic of research are methods that allow for efficient sampling from the posterior, with MCMC methods being often in the focus of attention (see for instance [63, 62, 64, 118, 80]).

Machine learning models that either learn the prior explicitly (see Section 3.2) or implicitly (see Section 3.1) can usually directly be extended towards uncertainty quantification, at least if sampling is computationally feasible. Uncertainty quantification in this context

typically means to compute pixel-wise marginal variances and regard them as indicator for uncertainty, see for instance [206, 207]. Generator-based priors, i.e., priors where the image manifold is described via a network $\mathcal{N}_\theta(z)$ with trained parameters and the latent variable z following a specified prior distribution, are analyzed in a Bayesian context for example in [94] (see also [71] for a related approach which, however, focuses on robust MAP estimation). The work [94] shows well-posedness of the posterior resulting from the incorporation of a learned, generator-based prior and also the existence of posterior moments, which can be sampled with MCMC techniques. Exploiting low dimensionality of the latent space, uncertainty can be visualized in this context via considering the covariance matrix for the latent variable, and mapping forward information on the principal components of this matrix to image space.

In [136] the authors impose a prior distribution $p(\theta)$ on the parameters θ of a learned regularizer $\mathcal{R}(u) = \mathcal{N}_\theta(u)$. That is, instead of estimating θ directly, in a Bayesian fashion they try to infer the distribution of θ . Subsequently, this allows to quantify the uncertainty with respect to the optimal parameters θ . The authors provide experiments with the TDV prior [113].

The work [165] uses Markov chain dropout to derive uncertainty estimates for deep-learning-based MRI reconstruction, and also qualitatively relates uncertainty to the reconstruction error. The work [148] uses a denoising autoencoder to approximate the gradient of the prior distribution in a Bayesian setting for MRI imaging, and combines this with sampling techniques to assess the uncertainty of particular features of the reconstructed images. Also in the context of Bayesian MR imaging, the work [126] uses diffusion models both for reconstruction and for the computation of uncertainty maps via sampling.

Also plug and play methods were recently extended to allow for uncertainty quantification. In [118] for instance, the authors use Tweedies formula to re-interpret the gradient of the log-prior, appearing in sampling algorithms, as MMSE denoiser, which opens the door to again perform sampling of a posterior distribution implicitly described by pre-trained denoisers. The work [118] analyzes this approach, in particular w.r.t. convergence of the resulting algorithms, and uses sampling to compute pixel-wise marginal posterior standard deviation.

A limitation of classical Bayesian uncertainty quantification methods, in particular in connection with learned, deep-neural-network-based priors, is that quantitative guarantees, such as error bounds that hold with high probability, can hardly be rigorously ensured. There are manifold reasons for this: It is hard to know or quantify the discrepancy between the true prior and the one learned on a finite sample; even in the idealized case of sufficient training samples, non-convexity of learning problems with deep neural networks usually prevent guarantees that the global minimum of the loss was found; and even if the prior was trained perfectly, sampling algorithms such as Langevin sampling usually require log-concave densities [62], which is not the case for deep-network-based models. The works [11, 137] consider an alternative strategy towards uncertainty quantification for inverse imaging problems, which is not directly affected by these limitations. Building on techniques of conformal prediction from [154], the main idea of [11, 137] is to develop machine-learning-based predictors for error intervals, but to regard them as black-box predictors and use

calibration data together with quantile estimates to obtain corrected versions of those predictors, whose error bounds are valid with high probability independent on assumptions on the underlying data distribution. Specifically, [137] considers the following setting: Assume we are given a learned prior and a specific inverse problem. Given an iid *calibration* data set $(u_i, y_i)_i$, we can use the prior to compute point estimates \hat{u}_i of u_i as well as estimates of the posterior variances $v_i = \mathbb{V}[u|y = y_i]$. The labeled data set then allows to estimate the relation between v_i and the error $\hat{u}_i - u_i$. Given a new unseen observation y_{new} we can compute $v_{\text{new}} = \mathbb{V}[u|y = y_{\text{new}}]$ and estimate the reconstruction error based on the learned relation between posterior variance and error. In [137] (relying on results of [154]) it is proven that the obtained error estimates hold with high probability (the probability taken over calibration data set, new observation y and the estimate of u), independent of assumptions on the data distribution or sampling algorithms.

REFERENCES

- [1] Moloud Abdar, Farhad Pourpanah, Sadiq Hussain, Dana Rezazadegan, Li Liu, Mohammad Ghavamzadeh, Paul Fieguth, Xiaochun Cao, Abbas Khosravi, U Rajendra Acharya, et al. A review of uncertainty quantification in deep learning: Techniques, applications and challenges. *Information fusion*, 76:243–297, 2021.
- [2] Abdullah Abdullah, Martin Holler, Karl Kunisch, and Malena Sabate Landman. Latent-space disentanglement with untrained generator networks for the isolation of different motion types in video data. In *International Conference on Scale Space and Variational Methods in Computer Vision*, pages 326–338. Springer, 2023.
- [3] Jonas Adler and Ozan Öktem. Solving ill-posed inverse problems using iterative deep neural networks. *Inverse Problems*, 33(12):124007, 2017.
- [4] Jonas Adler and Ozan Öktem. Learned primal-dual reconstruction. *IEEE Transactions on Medical Imaging*, 37(6):1322–1332, 2018.
- [5] Guillaume Alain and Yoshua Bengio. What regularized auto-encoders learn from the data-generating distribution. *The Journal of Machine Learning Research*, 15(1):3563–3593, 2014.
- [6] Giovanni S Alberti, Ernesto De Vito, Matti Lassas, Luca Ratti, and Matteo Santacesaria. Learning the optimal tikhonov regularizer for inverse problems. *Advances in Neural Information Processing Systems*, 34:25205–25216, 2021.
- [7] Giovanni S Alberti, Matteo Santacesaria, and Silvia Sciotto. Continuous generative neural networks. *arXiv preprint arXiv:2205.14627*, 2022.
- [8] Fabian Altekrüger, Alexander Denker, Paul Hagemann, Johannes Hertrich, Peter Maass, and Gabriele Steidl. Patchnr: Learning from small data by patch normalizing flow regularization. *arXiv preprint arXiv:2205.12021*, 2022.
- [9] Luigi Ambrosio, Nicola Fusco, and Diego Pallara. *Functions of Bounded Variation and Free Discontinuity Problems*. Oxford Mathematical Monographs, 2000.
- [10] Brian D.O. Anderson. Reverse-time diffusion equation models. *Stochastic Processes and their Applications*, 12(3):313–326, 1982.
- [11] Anastasios N Angelopoulos, Amit Pal Kohli, Stephen Bates, Michael Jordan, Jitendra Malik, Thayer Alshaabi, Srigokul Upadhyayula, and Yaniv Romano. Image-to-image regression with distribution-free uncertainty quantification and applications in imaging. In *International Conference on Machine Learning*, pages 717–730. PMLR, 2022.
- [12] Stephan Antholzer, Johannes Schwab, Johannes Bauer-Marschallinger, Peter Burgholzer, and Markus Haltmeier. NETT regularization for compressed sensing photoacoustic tomography. In Alexander A. Oraevsky and Lihong V. Wang, editors, *Photons Plus Ultrasound: Imaging and Sensing 2019*, volume 10878, page 108783B. International Society for Optics and Photonics, SPIE, 2019.

- [13] Siavash Arjomand Bigdeli, Matthias Zwicker, Paolo Favaro, and Meiguang Jin. Deep mean-shift priors for image restoration. In I. Guyon, U. Von Luxburg, S. Bengio, H. Wallach, R. Fergus, S. Vishwanathan, and R. Garnett, editors, *Advances in Neural Information Processing Systems*, volume 30. Curran Associates, Inc., 2017.
- [14] Martin Arjovsky, Soumith Chintala, and Léon Bottou. Wasserstein generative adversarial networks. In Doina Precup and Yee Whye Teh, editors, *Proceedings of the 34th International Conference on Machine Learning*, volume 70 of *Proceedings of Machine Learning Research*, pages 214–223. PMLR, 2017.
- [15] Clemens Arndt. Regularization theory of the analytic deep prior approach. *Inverse Problems*, 38(11):115005, 2022.
- [16] Clemens Arndt, Alexander Denker, Sören Dittmer, Nick Heilenkötter, Meira Iske, Tobias Kluth, Peter Maass, and Judith Nickel. Invertible residual networks in the context of regularization theory for linear inverse problems. *arXiv preprint arXiv:2306.01335*, 2023.
- [17] Simon Arridge, Peter Maass, Ozan Öktem, and Carola-Bibiane Schönlieb. Solving inverse problems using data-driven models. *Acta Numerica*, 28:1–174, 2019.
- [18] Muhammad Asim, Max Daniels, Oscar Leong, Ali Ahmed, and Paul Hand. Invertible generative models for inverse problems: mitigating representation error and dataset bias. In Hal Daumé III and Aarti Singh, editors, *Proceedings of the 37th International Conference on Machine Learning*, volume 119 of *Proceedings of Machine Learning Research*, pages 399–409. PMLR, 2020.
- [19] Muhammad Asim, Fahad Shamshad, and Ali Ahmed. Solving bilinear inverse problems using deep generative priors. *CoRR*, abs/1802.04073, 3(4):8, 2018.
- [20] Muhammad Asim, Fahad Shamshad, and Ali Ahmed. Blind image deconvolution using deep generative priors. *IEEE Transactions on Computational Imaging*, 6:1493–1506, 2020.
- [21] Andrea Aspri, Sebastian Banert, Ozan Öktem, and Otmar Scherzer. A data-driven iteratively regularized landweber iteration. *Numerical Functional Analysis and Optimization*, 41(10):1190–1227, 2020.
- [22] Andrea Aspri, Yury Korolev, and Otmar Scherzer. Data driven regularization by projection. *Inverse Problems*, 36(12):125009, 2020.
- [23] Andrea Aspri and Otmar Scherzer. Analysis of generalized iteratively regularized landweber iterations driven by data. *arXiv preprint arXiv:2312.03337*, 2023.
- [24] Francis Bach. Breaking the curse of dimensionality with convex neural networks. *The Journal of Machine Learning Research*, 18(1):629–681, 2017.
- [25] Yanna Bai, Wei Chen, Jie Chen, and Weisi Guo. Deep learning methods for solving linear inverse problems: Research directions and paradigms. *Signal Processing*, 177:107729, 2020.
- [26] Lorenzo Baldassari, Ali Siahkoobi, Josselin Garnier, Knut Solna, and Maarten V de Hoop. Conditional score-based diffusion models for bayesian inference in infinite dimensions. *arXiv preprint arXiv:2305.19147*, 2023.
- [27] Amir Beck and Marc Teboulle. A fast iterative shrinkage-thresholding algorithm for linear inverse problems. *SIAM Journal on Imaging Sciences*, 2(1):183–202, 2009.
- [28] Julius Berner, Philipp Grohs, Gitta Kutyniok, and Philipp Petersen. The modern mathematics of deep learning. *arXiv preprint arXiv:2105.04026*, pages 86–114, 2021.
- [29] Siavash Arjomand Bigdeli and Matthias Zwicker. Image restoration using autoencoding priors. *arXiv preprint arXiv:1703.09964*, 2017.
- [30] Ashish Bora, Ajil Jalal, Eric Price, and Alexandros G Dimakis. Compressed sensing using generative models. In *International conference on machine learning*, pages 537–546. PMLR, 2017.
- [31] Stephen Boyd, Neal Parikh, Eric Chu, Borja Peleato, and Jonathan Eckstein. Distributed optimization and statistical learning via the alternating direction method of multipliers. *Foundations and Trends in Machine Learning*, 3(1):1–122, 2011.
- [32] Kristian Bredies and Martin Holler. Higher-order total variation approaches and generalisations. *Inverse Problems. Topical Review*, 36(12):123001, 2020.

- [33] Kristian Bredies, Karl Kunisch, and Thomas Pock. Total generalized variation. *SIAM Journal on Imaging Sciences*, 3(3):492–526, 2010.
- [34] Kristian Bredies and Dirk A. Lorenz. Linear convergence of iterative soft-thresholding. *Journal of Fourier Analysis and Applications*, 14(5):813–837, 2008.
- [35] Alon Brifman, Yaniv Romano, and Michael Elad. Turning a denoiser into a super-resolver using plug and play priors. In *2016 IEEE International Conference on Image Processing (ICIP)*, pages 1404–1408, 2016.
- [36] A. Buades, B. Coll, and J.-M. Morel. A non-local algorithm for image denoising. In *2005 IEEE Computer Society Conference on Computer Vision and Pattern Recognition (CVPR'05)*, volume 2, pages 60–65 vol. 2, 2005.
- [37] Nathan Buskucic, Jalal Fadili, and Yvain Quéau. Convergence and recovery guarantees of unsupervised neural networks for inverse problems. *arXiv preprint arXiv:2309.12128*, 2023.
- [38] Antonin Chambolle and Thomas Pock. A first-order primal-dual algorithm for convex problems with applications to imaging. *Journal of Mathematical Imaging and Vision*, 40(1):120–145, 2011.
- [39] Stanley H. Chan, Xiran Wang, and Omar A. Elgendy. Plug-and-play admm for image restoration: Fixed-point convergence and applications. *IEEE Transactions on Computational Imaging*, 3(1):84–98, 2017.
- [40] George H-G. Chen and R. T. Rockafellar. Convergence rates in forward–backward splitting. *SIAM Journal on Optimization*, 7(2):421–444, 1997.
- [41] Hu Chen, Yi Zhang, Mannudeep K. Kalra, Feng Lin, Yang Chen, Peixi Liao, Jiliu Zhou, and Ge Wang. Low-dose ct with a residual encoder-decoder convolutional neural network. *IEEE Transactions on Medical Imaging*, 36(12):2524–2535, 2017.
- [42] Tianping Chen and Hong Chen. Universal approximation to nonlinear operators by neural networks with arbitrary activation functions and its application to dynamical systems. *IEEE transactions on neural networks*, 6(4):911–917, 1995.
- [43] Yunjin Chen and Thomas Pock. Trainable nonlinear reaction diffusion: A flexible framework for fast and effective image restoration. *IEEE Transactions on Pattern Analysis and Machine Intelligence*, 39(6):1256–1272, 2017.
- [44] Zezhou Cheng, Matheus Gadelha, Subhansu Maji, and Daniel Sheldon. A bayesian perspective on the deep image prior. In *Proceedings of the IEEE/CVF Conference on Computer Vision and Pattern Recognition*, pages 5443–5451, 2019.
- [45] Hyungjin Chung, Jeongsol Kim, Sehui Kim, and Jong Chul Ye. Parallel diffusion models of operator and image for blind inverse problems. In *Proceedings of the IEEE/CVF Conference on Computer Vision and Pattern Recognition (CVPR)*, pages 6059–6069, 2023.
- [46] Hyungjin Chung, Jeongsol Kim, Michael T Mccann, Marc L Klasky, and Jong Chul Ye. Diffusion posterior sampling for general noisy inverse problems. *arXiv preprint arXiv:2209.14687*, 2022.
- [47] Hyungjin Chung, Byeongsu Sim, Dohoon Ryu, and Jong Chul Ye. Improving diffusion models for inverse problems using manifold constraints. In S. Koyejo, S. Mohamed, A. Agarwal, D. Belgrave, K. Cho, and A. Oh, editors, *Advances in Neural Information Processing Systems*, volume 35, pages 25683–25696. Curran Associates, Inc., 2022.
- [48] Hyungjin Chung, Byeongsu Sim, and Jong Chul Ye. Come-closer-diffuse-faster: Accelerating conditional diffusion models for inverse problems through stochastic contraction. In *Proceedings of the IEEE/CVF Conference on Computer Vision and Pattern Recognition (CVPR)*, pages 12413–12422, 2022.
- [49] Hyungjin Chung and Jong Chul Ye. Score-based diffusion models for accelerated MRI. *Medical Image Analysis*, 80:102479, 2022.
- [50] Regev Cohen, Michael Elad, and Peyman Milanfar. Regularization by denoising via fixed-point projection (red-pro). *SIAM Journal on Imaging Sciences*, 14(3):1374–1406, 2021.

- [51] Kostadin Dabov, Alessandro Foi, Vladimir Katkovnik, and Karen Egiazarian. Image denoising by sparse 3-d transform-domain collaborative filtering. *IEEE Transactions on Image Processing*, 16(8):2080–2095, 2007.
- [52] Mohammad Zalbagi Darestani and Reinhard Heckel. Accelerated MRI with un-trained neural networks. *IEEE Transactions on Computational Imaging*, 7:724–733, 2021.
- [53] Ingrid Daubechies, Michel Defrise, and Christine De Mol. An iterative thresholding algorithm for linear inverse problems with a sparsity constraint. *Communications on Pure and Applied Mathematics*, 57(11):1413–1457, 2004.
- [54] J.C. De Los Reyes, C.-B. Schönlieb, and T. Valkonen. The structure of optimal parameters for image restoration problems. *Journal of Mathematical Analysis and Applications*, 434(1):464–500, 2016.
- [55] Manik Dhar, Aditya Grover, and Stefano Ermon. Modeling sparse deviations for compressed sensing using generative models. In Jennifer Dy and Andreas Krause, editors, *Proceedings of the 35th International Conference on Machine Learning*, volume 80 of *Proceedings of Machine Learning Research*, pages 1214–1223. PMLR, 2018.
- [56] Laurent Dinh, David Krueger, and Yoshua Bengio. NICE: non-linear independent components estimation. In Yoshua Bengio and Yann LeCun, editors, *3rd International Conference on Learning Representations, ICLR 2015, San Diego, CA, USA, May 7-9, 2015, Workshop Track Proceedings*, 2015.
- [57] Laurent Dinh, Jascha Sohl-Dickstein, and Samy Bengio. Density estimation using real NVP. In *5th International Conference on Learning Representations, ICLR 2017, Toulon, France, April 24-26, 2017, Conference Track Proceedings*. OpenReview.net, 2017.
- [58] Sören Dittmer, Tobias Kluth, Peter Maass, and Daniel Otero Baguer. Regularization by architecture: A deep prior approach for inverse problems. *Journal of Mathematical Imaging and Vision*, 62:456–470, 2020.
- [59] Weisheng Dong, Peiyao Wang, Wotao Yin, Guangming Shi, Fangfang Wu, and Xiaotong Lu. Denoising prior driven deep neural network for image restoration. *IEEE Transactions on Pattern Analysis and Machine Intelligence*, 41(10):2305–2318, 2019.
- [60] Margaret Duff, Neill DF Campbell, and Matthias J Ehrhardt. Regularising inverse problems with generative machine learning models. *arXiv preprint arXiv:2107.11191*, 2021.
- [61] Margaret Duff, Ivor Simpson, Matthias J Ehrhardt, and Neill DF Campbell. VAEs with structured image covariance applied to compressed sensing MRI. *Physics in Medicine & Biology*, 68(16):165008, 2023.
- [62] Alain Durmus, Szymon Majewski, and Błażej Miasojedow. Analysis of langevin monte carlo via convex optimization. *The Journal of Machine Learning Research*, 20(1):2666–2711, 2019.
- [63] Alain Durmus and Éric Moulines. High-dimensional Bayesian inference via the unadjusted Langevin algorithm. *Bernoulli*, 25(4A):2854 – 2882, 2019.
- [64] Alain Durmus, Éric Moulines, and Marcelo Pereyra. A proximal markov chain monte carlo method for bayesian inference in imaging inverse problems: When langevin meets moreau. *SIAM Review*, 64(4):991–1028, 2022.
- [65] Andrea Ebner and Markus Haltmeier. Plug-and-play image reconstruction is a convergent regularization method. *arXiv preprint arXiv:2212.06881*, 2022.
- [66] Bradley Efron. Tweedie’s formula and selection bias. *Journal of the American Statistical Association*, 106(496):1602–1614, 2011. PMID: 22505788.
- [67] Michael Elad and Michal Aharon. Image denoising via sparse and redundant representations over learned dictionaries. *IEEE Transactions on Image Processing*, 15(12):3736–3745, 2006.
- [68] Heinz Werner Engl and Martin Hanke. *Regularization of inverse problems*, volume 375. Springer Science & Business Media, 1996.
- [69] Moritz Erlacher and Martin Zach. Joint non-linear MRI inversion with diffusion priors. *arXiv preprint arXiv:2310.14842*, 2023.

- [70] Guangyu Gao, Bo Han, Zhenwu Fu, and Shanshan Tong. A fast data-driven iteratively regularized method with convex penalty for solving ill-posed problems. *SIAM Journal on Imaging Sciences*, 16(2):640–670, 2023.
- [71] Mario González, Andrés Almansa, and Pauline Tan. Solving inverse problems by joint posterior maximization with autoencoding prior. *SIAM Journal on Imaging Sciences*, 15(2):822–859, 2022.
- [72] Ian Goodfellow, Jean Pouget-Abadie, Mehdi Mirza, Bing Xu, David Warde-Farley, Sherjil Ozair, Aaron Courville, and Yoshua Bengio. Generative adversarial nets. In Z. Ghahramani, M. Welling, C. Cortes, N. Lawrence, and K.Q. Weinberger, editors, *Advances in Neural Information Processing Systems*, volume 27. Curran Associates, Inc., 2014.
- [73] Karol Gregor and Yann LeCun. Learning fast approximations of sparse coding. In *Proceedings of the 27th International Conference on International Conference on Machine Learning*, ICML’10, page 399–406, Madison, WI, USA, 2010. Omnipress.
- [74] Yu Guan, Zongjiang Tu, Shanshan Wang, Yuhao Wang, Qiegen Liu, and Dong Liang. Magnetic resonance imaging reconstruction using a deep energy-based model. *NMR in Biomedicine*, 36(3):e4848, 2023.
- [75] Ishaan Gulrajani, Faruk Ahmed, Martin Arjovsky, Vincent Dumoulin, and Aaron C Courville. Improved training of wasserstein GANs. In I. Guyon, U. Von Luxburg, S. Bengio, H. Wallach, R. Fergus, S. Vishwanathan, and R. Garnett, editors, *Advances in Neural Information Processing Systems*, volume 30. Curran Associates, Inc., 2017.
- [76] Bichuan Guo, Yuxing Han, and Jiangtao Wen. Agem: Solving linear inverse problems via deep priors and sampling. In H. Wallach, H. Larochelle, A. Beygelzimer, F. d’Alché-Buc, E. Fox, and R. Garnett, editors, *Advances in Neural Information Processing Systems*, volume 32. Curran Associates, Inc., 2019.
- [77] Javier Gurrola-Ramos, Oscar Dalmau, and Teresa E. Alarcón. A residual dense u-net neural network for image denoising. *IEEE Access*, 9:31742–31754, 2021.
- [78] Andreas Habring and Martin Holler. A generative variational model for inverse problems in imaging. *SIAM Journal on Mathematics of Data Science*, 4(1):306–335, 2022.
- [79] Andreas Habring and Martin Holler. A note on the regularity of images generated by convolutional neural networks. *SIAM Journal on Mathematics of Data Science*, 5(3):670–692, 2023.
- [80] Andreas Habring, Martin Holler, and Thomas Pock. Subgradient langevin methods for sampling from non-smooth potentials. *arXiv preprint arXiv:2308.01417*, 2023.
- [81] Paul Hagemann, Lars Ruthotto, Gabriele Steidl, and Nicole Tianjiao Yang. Multilevel diffusion: Infinite dimensional score-based diffusion models for image generation. *arXiv preprint arXiv:2303.04772*, 2023.
- [82] Markus Haltmeier, Richard Kowar, and Markus Tiefertaler. Data-driven Morozov regularization of inverse problems. *arXiv preprint arXiv:2310.14290*, 2023.
- [83] Kerstin Hammernik, Teresa Klatzer, Erich Kobler, Michael P. Recht, Daniel K. Sodickson, Thomas Pock, and Florian Knoll. Learning a variational network for reconstruction of accelerated MRI data. *Magnetic Resonance in Medicine*, 79(6):3055–3071, 2018.
- [84] Paul Hand, Oscar Leong, and Vlad Voroninski. Phase retrieval under a generative prior. In S. Bengio, H. Wallach, H. Larochelle, K. Grauman, N. Cesa-Bianchi, and R. Garnett, editors, *Advances in Neural Information Processing Systems*, volume 31. Curran Associates, Inc., 2018.
- [85] Marzieh Hasannasab, Johannes Hertrich, Sebastian Neumayer, Gerlind Plonka, Simon Setzer, and Gabriele Steidl. Parseval proximal neural networks. *Journal of Fourier Analysis and Applications*, 26:1–31, 2020.
- [86] Ji He, Yan Yang, Yongbo Wang, Dong Zeng, Zhaoying Bian, Hao Zhang, Jian Sun, Zongben Xu, and Jianhua Ma. Optimizing a parameterized plug-and-play admm for iterative low-dose ct reconstruction. *IEEE Transactions on Medical Imaging*, 38(2):371–382, 2019.
- [87] Reinhard Heckel. Regularizing linear inverse problems with convolutional neural networks. *arXiv preprint arXiv:1907.03100*, 2019.

- [88] Reinhard Heckel and Paul Hand. Deep decoder: Concise image representations from untrained non-convolutional networks. *arXiv preprint arXiv:1810.03982*, 2018.
- [89] Reinhard Heckel and Mahdi Soltanolkotabi. Denoising and regularization via exploiting the structural bias of convolutional generators. *arXiv preprint arXiv:1910.14634*, 2019.
- [90] Reinhard Heckel and Mahdi Soltanolkotabi. Compressive sensing with un-trained neural networks: Gradient descent finds a smooth approximation. In *International Conference on Machine Learning*, pages 4149–4158. PMLR, 2020.
- [91] Allard Adriaan Hendriksen, Daniël Maria Pelt, and K. Joost Batenburg. Noise2inverse: Self-supervised deep convolutional denoising for tomography. *IEEE Transactions on Computational Imaging*, 6:1320–1335, 2020.
- [92] Geoffrey E. Hinton. Training products of experts by minimizing contrastive divergence. *Neural Computation*, 14(8):1771–1800, 2002.
- [93] Jonathan Ho, Ajay Jain, and Pieter Abbeel. Denoising diffusion probabilistic models. In H. Larochelle, M. Ranzato, R. Hadsell, M.F. Balcan, and H. Lin, editors, *Advances in Neural Information Processing Systems*, volume 33, pages 6840–6851. Curran Associates, Inc., 2020.
- [94] Matthew Holden, Marcelo Pereyra, and Konstantinos C Zygalakis. Bayesian imaging with data-driven priors encoded by neural networks. *SIAM Journal on Imaging Sciences*, 15(2):892–924, 2022.
- [95] Tao Hong, Yaniv Romano, and Michael Elad. Acceleration of red via vector extrapolation. *Journal of Visual Communication and Image Representation*, 63:102575, 2019.
- [96] Chang Min Hyun, Hwa Pyung Kim, Sung Min Lee, Sungchul Lee, and Jin Keun Seo. Deep learning for undersampled MRI reconstruction. *Physics in Medicine & Biology*, 63(13):135007, 2018.
- [97] Aapo Hyvärinen. Estimation of non-normalized statistical models by score matching. *Journal of Machine Learning Research*, 6(24):695–709, 2005.
- [98] Phillip Isola, Jun-Yan Zhu, Tinghui Zhou, and Alexei A. Efros. Image-to-image translation with conditional adversarial networks. In *Proceedings of the IEEE Conference on Computer Vision and Pattern Recognition (CVPR)*, 2017.
- [99] Valentin Konstantinovich Ivanov. On linear problems which are not well-posed. *Doklady Akademii Nauk SSSR*, 145(2):270–272, 1962.
- [100] Gauri Jagatap and Chinmay Hegde. Algorithmic guarantees for inverse imaging with untrained network priors. *Advances in neural information processing systems*, 32, 2019.
- [101] Viren Jain and Sebastian Seung. Natural image denoising with convolutional networks. In D. Koller, D. Schuurmans, Y. Bengio, and L. Bottou, editors, *Advances in Neural Information Processing Systems*, volume 21. Curran Associates, Inc., 2008.
- [102] Kyong Hwan Jin, Michael T. McCann, Emmanuel Froustey, and Michael Unser. Deep convolutional neural network for inverse problems in imaging. *IEEE Transactions on Image Processing*, 26(9):4509–4522, 2017.
- [103] Samira Kabri, Alexander Auras, Danilo Riccio, Hartmut Bauermeister, Martin Benning, Michael Moeller, and Martin Burger. Convergent data-driven regularizations for ct reconstruction. *arXiv preprint arXiv:2212.07786*, 2022.
- [104] Ulugbek S. Kamilov, Hassan Mansour, and Brendt Wohlberg. A plug-and-play priors approach for solving nonlinear imaging inverse problems. *IEEE Signal Processing Letters*, 24(12):1872–1876, 2017.
- [105] Eunhee Kang, Junhong Min, and Jong Chul Ye. A deep convolutional neural network using directional wavelets for low-dose x-ray ct reconstruction. *Medical Physics*, 44(10):e360–e375, 2017.
- [106] Mahdi Karami, Dale Schuurmans, Jascha Sohl-Dickstein, Laurent Dinh, and Daniel Duckworth. Invertible convolutional flow. In H. Wallach, H. Larochelle, A. Beygelzimer, F. d'Alché-Buc, E. Fox, and R. Garnett, editors, *Advances in Neural Information Processing Systems*, volume 32. Curran Associates, Inc., 2019.
- [107] Bahjat Kwar, Michael Elad, Stefano Ermon, and Jiaming Song. Denoising diffusion restoration models. In S. Koyejo, S. Mohamed, A. Agarwal, D. Belgrave, K. Cho, and A. Oh, editors, *Advances*

- in Neural Information Processing Systems*, volume 35, pages 23593–23606. Curran Associates, Inc., 2022.
- [108] Bahjat Kawar, Gregory Vaksman, and Michael Elad. Snips: Solving noisy inverse problems stochastically. In M. Ranzato, A. Beygelzimer, Y. Dauphin, P.S. Liang, and J. Wortman Vaughan, editors, *Advances in Neural Information Processing Systems*, volume 34, pages 21757–21769. Curran Associates, Inc., 2021.
- [109] C. Kervrann and J. Boulanger. Optimal spatial adaptation for patch-based image denoising. *IEEE Transactions on Image Processing*, 15(10):2866–2878, 2006.
- [110] Diederik P. Kingma and Max Welling. Auto-encoding variational bayes. In Yoshua Bengio and Yann LeCun, editors, *2nd International Conference on Learning Representations, ICLR 2014, Banff, AB, Canada, April 14-16, 2014, Conference Track Proceedings*, 2014.
- [111] Durk P Kingma and Prafulla Dhariwal. Glow: Generative flow with invertible 1x1 convolutions. In S. Bengio, H. Wallach, H. Larochelle, K. Grauman, N. Cesa-Bianchi, and R. Garnett, editors, *Advances in Neural Information Processing Systems*, volume 31. Curran Associates, Inc., 2018.
- [112] Florian Knoll, Jure Zbontar, Anuroop Sriram, Matthew J Muckley, Mary Bruno, Aaron Defazio, Marc Parente, Krzysztof J Geras, Joe Katsnelson, Hersh Chandarana, et al. fastMRI: A publicly available raw k-space and DICOM dataset of knee images for accelerated MR image reconstruction using machine learning. *Radiology: Artificial Intelligence*, 2(1):e190007, 2020.
- [113] Erich Kobler, Alexander Effland, Karl Kunisch, and Thomas Pock. Total deep variation for linear inverse problems. In *Proceedings of the IEEE/CVF Conference on computer vision and pattern recognition*, pages 7549–7558, 2020.
- [114] Erich Kobler, Alexander Effland, Karl Kunisch, and Thomas Pock. Total deep variation: A stable regularization method for inverse problems. *IEEE Transactions on Pattern Analysis and Machine Intelligence*, 44(12):9163–9180, 2022.
- [115] Yury Korolev. Two-layer neural networks with values in a banach space. *SIAM Journal on Mathematical Analysis*, 54(6):6358–6389, 2022.
- [116] Karl Kunisch and Thomas Pock. A bilevel optimization approach for parameter learning in variational models. *SIAM Journal on Imaging Sciences*, 6(2):938–983, 2013.
- [117] Samuel Lanthaler, Siddhartha Mishra, and George E Karniadakis. Error estimates for deeponets: A deep learning framework in infinite dimensions. *Transactions of Mathematics and Its Applications*, 6(1):tnac001, 2022.
- [118] Rémi Laumont, Valentin De Bortoli, Andrés Almansa, Julie Delon, Alain Durmus, and Marcelo Pereyra. Bayesian imaging using plug & play priors: When langevin meets tweedie. *SIAM Journal on Imaging Sciences*, 15(2):701–737, 2022.
- [119] Jaakko Lehtinen, Jacob Munkberg, Jon Hasselgren, Samuli Laine, Tero Karras, Miika Aittala, and Timo Aila. Noise2Noise: Learning image restoration without clean data. In Jennifer Dy and Andreas Krause, editors, *Proceedings of the 35th International Conference on Machine Learning*, volume 80 of *Proceedings of Machine Learning Research*, pages 2965–2974. PMLR, 2018.
- [120] Housen Li, Johannes Schwab, Stephan Antholzer, and Markus Haltmeier. Nett: solving inverse problems with deep neural networks. *Inverse Problems*, 36(6):065005, 2020.
- [121] Y Li, Bruno Sixou, and F Peyrin. A review of the deep learning methods for medical images super resolution problems. *IRBM*, 42(2):120–133, 2021.
- [122] Jiaming Liu, Yu Sun, Xiaojian Xu, and Ulugbek S Kamilov. Image restoration using total variation regularized deep image prior. In *ICASSP 2019-2019 IEEE International Conference on Acoustics, Speech and Signal Processing (ICASSP)*, pages 7715–7719. Ieee, 2019.
- [123] Yilin Liu, Jiang Li, Yunkui Pang, Dong Nie, and Pew-Thian Yap. The devil is in the upsampling: Architectural decisions made simpler for denoising with deep image prior. In *Proceedings of the IEEE/CVF International Conference on Computer Vision (ICCV)*, pages 12408–12417, 2023.

- [124] Alice Lucas, Michael Iliadis, Rafael Molina, and Aggelos K Katsaggelos. Using deep neural networks for inverse problems in imaging: beyond analytical methods. *IEEE Signal Processing Magazine*, 35(1):20–36, 2018.
- [125] Sebastian Lunz, Ozan Öktem, and Carola-Bibiane Schönlieb. Adversarial regularizers in inverse problems. In S. Bengio, H. Wallach, H. Larochelle, K. Grauman, N. Cesa-Bianchi, and R. Garnett, editors, *Advances in Neural Information Processing Systems*, volume 31. Curran Associates, Inc., 2018.
- [126] Guanxiong Luo, Moritz Blumenthal, Martin Heide, and Martin Uecker. Bayesian MRI reconstruction with joint uncertainty estimation using diffusion models. *Magnetic Resonance in Medicine*, 90(1):295–311, 2023.
- [127] Julien Mairal, Francis Bach, Jean Ponce, Guillermo Sapiro, and Andrew Zisserman. Non-local sparse models for image restoration. In *2009 IEEE 12th International Conference on Computer Vision*, pages 2272–2279, 2009.
- [128] Gary Mataev, Peyman Milanfar, and Michael Elad. Deepred: Deep image prior powered by red. In *Proceedings of the IEEE/CVF International Conference on Computer Vision Workshops*, pages 0–0, 2019.
- [129] Michael T McCann, Kyong Hwan Jin, and Michael Unser. Convolutional neural networks for inverse problems in imaging: A review. *IEEE Signal Processing Magazine*, 34(6):85–95, 2017.
- [130] Tim Meinhardt, Michael Moller, Caner Hazirbas, and Daniel Cremers. Learning proximal operators: Using denoising networks for regularizing inverse imaging problems. In *Proceedings of the IEEE International Conference on Computer Vision (ICCV)*, 2017.
- [131] Christopher Metzler, Phillip Schniter, Ashok Veeraraghavan, and Richard Baraniuk. prDeep: Robust phase retrieval with a flexible deep network. In Jennifer Dy and Andreas Krause, editors, *Proceedings of the 35th International Conference on Machine Learning*, volume 80 of *Proceedings of Machine Learning Research*, pages 3501–3510. PMLR, 2018.
- [132] Jean-Jacques Moreau. Proximité et dualité dans un espace hilbertien. *Bulletin de la Société mathématique de France*, 93:273–299, 1965.
- [133] Lukas Mosser, Olivier Dubrule, and Martin J. Blunt. Stochastic seismic waveform inversion using generative adversarial networks as a geological prior. *Mathematical Geosciences*, 52(1):53–79, 2020.
- [134] Subhadip Mukherjee, Sören Dittmer, Zakhar Shumaylov, Sebastian Lunz, Ozan Öktem, and Carola-Bibiane Schönlieb. Learned convex regularizers for inverse problems. *arXiv preprint arXiv:2008.02839*, 2020.
- [135] Subhadip Mukherjee, Andreas Hauptmann, Ozan Öktem, Marcelo Pereyra, and Carola-Bibiane Schönlieb. Learned reconstruction methods with convergence guarantees: a survey of concepts and applications. *IEEE Signal Processing Magazine*, 40(1):164–182, 2023.
- [136] Dominik Narnhofer, Alexander Effland, Erich Kobler, Kerstin Hammernik, Florian Knoll, and Thomas Pock. Bayesian uncertainty estimation of learned variational MRI reconstruction. *IEEE Transactions on Medical Imaging*, 41(2):279–291, 2022.
- [137] Dominik Narnhofer, Andreas Habring, Martin Holler, and Thomas Pock. Posterior-variance-based error quantification for inverse problems in imaging. *arXiv preprint arXiv:2212.12499*, 2022.
- [138] Daniel Obmann, Linh Nguyen, Johannes Schwab, and Markus Haltmeier. Augmented nett regularization of inverse problems. *Journal of Physics Communications*, 5(10):105002, 2021.
- [139] Daniel Obmann, Johannes Schwab, and Markus Haltmeier. Deep synthesis network for regularizing inverse problems. *Inverse Problems*, 37(1):015005, 2020.
- [140] Gregory Ongie, Ajil Jalal, Christopher A Metzler, Richard G Baraniuk, Alexandros G Dimakis, and Rebecca Willett. Deep learning techniques for inverse problems in imaging. *IEEE Journal on Selected Areas in Information Theory*, 1(1):39–56, 2020.
- [141] Xingang Pan, Xiaohang Zhan, Bo Dai, Dahua Lin, Chen Change Loy, and Ping Luo. Exploiting deep generative prior for versatile image restoration and manipulation. *IEEE Transactions on Pattern Analysis and Machine Intelligence*, 44(11):7474–7489, 2022.

- [142] Daniël M. Pelt, Kees Joost Batenburg, and James A. Sethian. Improving tomographic reconstruction from limited data using mixed-scale dense convolutional neural networks. *Journal of Imaging*, 4(11), 2018.
- [143] Patrick Putzky and Max Welling. Recurrent inference machines for solving inverse problems. *arXiv preprint arXiv:1706.04008*, 2017.
- [144] Adnan Qayyum, Inaam Ilahi, Fahad Shamshad, Farid Boussaid, Mohammed Bennamoun, and Junaid Qadir. Untrained neural network priors for inverse imaging problems: A survey. *IEEE Transactions on Pattern Analysis and Machine Intelligence*, 2022.
- [145] Tran Minh Quan, Thanh Nguyen-Duc, and Won-Ki Jeong. Compressed sensing MRI reconstruction using a generative adversarial network with a cyclic loss. *IEEE Transactions on Medical Imaging*, 37(6):1488–1497, 2018.
- [146] Alec Radford, Luke Metz, and Soumith Chintala. Unsupervised representation learning with deep convolutional generative adversarial networks. In Yoshua Bengio and Yann LeCun, editors, *4th International Conference on Learning Representations, ICLR 2016, San Juan, Puerto Rico, May 2-4, 2016, Conference Track Proceedings*, 2016.
- [147] Ankit Raj, Yuqi Li, and Yoram Bresler. Gan-based projector for faster recovery with convergence guarantees in linear inverse problems. In *Proceedings of the IEEE/CVF International Conference on Computer Vision (ICCV)*, 2019.
- [148] Zaccharie Ramzi, Benjamin Remy, Francois Lanasse, Jean-Luc Starck, and Philippe Ciuciu. Denoising score-matching for uncertainty quantification in inverse problems. *arXiv preprint arXiv:2011.08698*, 2020.
- [149] Edward T. Reehorst and Philip Schniter. Regularization by denoising: Clarifications and new interpretations. *IEEE Transactions on Computational Imaging*, 5(1):52–67, 2019.
- [150] Danilo Rezende and Shakir Mohamed. Variational inference with normalizing flows. In Francis Bach and David Blei, editors, *Proceedings of the 32nd International Conference on Machine Learning*, volume 37 of *Proceedings of Machine Learning Research*, pages 1530–1538, Lille, France, 2015. PMLR.
- [151] J. H. Rick Chang, Chun-Liang Li, Barnabas Poczos, B. V. K. Vijaya Kumar, and Aswin C. Sankaranarayanan. One network to solve them all – solving linear inverse problems using deep projection models. In *Proceedings of the IEEE International Conference on Computer Vision (ICCV)*, 2017.
- [152] Gabrio Rizzuti, Ali Siahkoochi, Philipp A. Witte, and Felix J. Herrmann. Parameterizing uncertainty by deep invertible networks: An application to reservoir characterization. In *SEG International Exposition and Annual Meeting*, page D031S057R006, 2020.
- [153] Yaniv Romano, Michael Elad, and Peyman Milanfar. The little engine that could: Regularization by denoising (red). *SIAM Journal on Imaging Sciences*, 10(4):1804–1844, 2017.
- [154] Yaniv Romano, Evan Patterson, and Emmanuel Candes. Conformalized quantile regression. *Advances in neural information processing systems*, 32, 2019.
- [155] Olaf Ronneberger, Philipp Fischer, and Thomas Brox. U-net: Convolutional networks for biomedical image segmentation. In *International Conference on Medical image computing and computer-assisted intervention*, pages 234–241. Springer, 2015.
- [156] Stefan Roth and Michael J Black. Fields of experts: A framework for learning image priors. In *2005 IEEE Computer Society Conference on Computer Vision and Pattern Recognition (CVPR'05)*, volume 2, pages 860–867. IEEE, 2005.
- [157] Stefan Roth and Michael J Black. Fields of experts. *International Journal of Computer Vision*, 82(2):205–229, 2009.
- [158] Leonid I Rudin, Stanley Osher, and Emad Fatemi. Nonlinear total variation based noise removal algorithms. *Physica D: nonlinear phenomena*, 60(1-4):259–268, 1992.
- [159] Leonid I. Rudin, Stanley Osher, and Emad Fatemi. Nonlinear total variation based noise removal algorithms. *Physica D*, 60(1–4):259–268, 1992.
- [160] Ernest Ryu, Jialin Liu, Sicheng Wang, Xiaohan Chen, Zhangyang Wang, and Wotao Yin. Plug-and-play methods provably converge with properly trained denoisers. In Kamalika Chaudhuri and

- Ruslan Salakhutdinov, editors, *Proceedings of the 36th International Conference on Machine Learning*, volume 97 of *Proceedings of Machine Learning Research*, pages 5546–5557. PMLR, 2019.
- [161] Jonathan Scarlett, Reinhard Heckel, Miguel RD Rodrigues, Paul Hand, and Yonina C Eldar. Theoretical perspectives on deep learning methods in inverse problems. *IEEE journal on selected areas in information theory*, 3(3):433–453, 2022.
- [162] Otmar Scherzer, Markus Grasmair, Harald Grossauer, Markus Haltmeier, and Frank Lenzen. *Variational Methods in Imaging*, volume 167. Springer Science & Business Media, 2008.
- [163] Otmar Scherzer, Bernd Hofmann, and Zuhair Nashed. Gauss–newton method for solving linear inverse problems with neural network coders. *Sampling Theory, Signal Processing, and Data Analysis*, 21(2):25, 2023.
- [164] Jo Schlemper, Jose Caballero, Joseph V. Hajnal, Anthony N. Price, and Daniel Rueckert. A deep cascade of convolutional neural networks for dynamic mr image reconstruction. *IEEE Transactions on Medical Imaging*, 37(2):491–503, 2018.
- [165] Jo Schlemper, Daniel C Castro, Wenjia Bai, Chen Qin, Ozan Oktay, Jinming Duan, Anthony N Price, Jo Hajnal, and Daniel Rueckert. Bayesian deep learning for accelerated mr image reconstruction. In *Machine Learning for Medical Image Reconstruction: First International Workshop, MLMIR 2018, Held in Conjunction with MICCAI 2018, Granada, Spain, September 16, 2018, Proceedings 1*, pages 64–71. Springer, 2018.
- [166] Johannes Schwab, Stephan Antholzer, and Markus Haltmeier. Deep null space learning for inverse problems: convergence analysis and rates. *Inverse Problems*, 35(2):025008, 2019.
- [167] Johannes Schwab, Stephan Antholzer, and Markus Haltmeier. Big in japan: Regularizing networks for solving inverse problems. *Journal of mathematical imaging and vision*, 62(3):445–455, 2020.
- [168] Ortal Senouf, Sanketh Vedula, Tomer Weiss, Alex Bronstein, Oleg Michailovich, and Michael Zibulevsky. Self-supervised learning of inverse problem solvers in medical imaging. In Qian Wang, Fausto Milletari, Hien V. Nguyen, Shadi Albarqouni, M. Jorge Cardoso, Nicola Rieke, Ziyue Xu, Konstantinos Kamnitsas, Vishal Patel, Badri Roysam, Steve Jiang, Kevin Zhou, Khoa Luu, and Ngan Le, editors, *Domain Adaptation and Representation Transfer and Medical Image Learning with Less Labels and Imperfect Data*, pages 111–119, Cham, 2019. Springer International Publishing.
- [169] Jin Keun Seo, Kang Cheol Kim, Ariungerel Jargal, Kyoungun Lee, and Bastian Harrach. A learning-based method for solving ill-posed nonlinear inverse problems: A simulation study of lung eit. *SIAM Journal on Imaging Sciences*, 12(3):1275–1295, 2019.
- [170] Viraj Shah and Chinmay Hegde. Solving linear inverse problems using gan priors: An algorithm with provable guarantees. In *2018 IEEE International Conference on Acoustics, Speech and Signal Processing (ICASSP)*, pages 4609–4613, 2018.
- [171] Nir Shlezinger, Jay Whang, Yonina C Eldar, and Alexandros G Dimakis. Model-based deep learning. *Proceedings of the IEEE*, 2023.
- [172] Ali Siahkoobi, Gabrio Rizzuti, Philipp A Witte, and Felix J Herrmann. Faster uncertainty quantification for inverse problems with conditional normalizing flows. *arXiv preprint arXiv:2007.07985*, 2020.
- [173] Jascha Sohl-Dickstein, Eric Weiss, Niru Maheswaranathan, and Surya Ganguli. Deep unsupervised learning using nonequilibrium thermodynamics. In Francis Bach and David Blei, editors, *Proceedings of the 32nd International Conference on Machine Learning*, volume 37 of *Proceedings of Machine Learning Research*, pages 2256–2265, Lille, France, 2015. PMLR.
- [174] Yang Song and Stefano Ermon. Generative modeling by estimating gradients of the data distribution. In H. Wallach, H. Larochelle, A. Beygelzimer, F. d'Alché-Buc, E. Fox, and R. Garnett, editors, *Advances in Neural Information Processing Systems*, volume 32. Curran Associates, Inc., 2019.
- [175] Yang Song, Sahaj Garg, Jiaxin Shi, and Stefano Ermon. Sliced score matching: A scalable approach to density and score estimation. In Ryan P. Adams and Vibhav Gogate, editors, *Proceedings of The 35th Uncertainty in Artificial Intelligence Conference*, volume 115 of *Proceedings of Machine Learning Research*, pages 574–584. PMLR, 2020.

- [176] Yang Song, Liyue Shen, Lei Xing, and Stefano Ermon. Solving inverse problems in medical imaging with score-based generative models. *arXiv preprint arXiv:2111.08005*, 2021.
- [177] Yang Song, Jascha Sohl-Dickstein, Diederik P Kingma, Abhishek Kumar, Stefano Ermon, and Ben Poole. Score-based generative modeling through stochastic differential equations. *arXiv preprint arXiv:2011.13456*, 2020.
- [178] Suhas Sreehari, S. V. Venkatakrishnan, Brendt Wohlberg, Gregory T. Buzzard, Lawrence F. Drummy, Jeffrey P. Simmons, and Charles A. Bouman. Plug-and-play priors for bright field electron tomography and sparse interpolation. *IEEE Transactions on Computational Imaging*, 2(4):408–423, 2016.
- [179] Andrew M Stuart. Inverse problems: a bayesian perspective. *Acta numerica*, 19:451–559, 2010.
- [180] He Sun and Katherine L. Bouman. Deep probabilistic imaging: Uncertainty quantification and multi-modal solution characterization for computational imaging. *Proceedings of the AAAI Conference on Artificial Intelligence*, 35(3):2628–2637, 2021.
- [181] Yu Sun, Jiaming Liu, and Ulugbek Kamilov. Block coordinate regularization by denoising. In H. Wallach, H. Larochelle, A. Beygelzimer, F. d'Alché-Buc, E. Fox, and R. Garnett, editors, *Advances in Neural Information Processing Systems*, volume 32. Curran Associates, Inc., 2019.
- [182] Yu Sun, Brendt Wohlberg, and Ulugbek S. Kamilov. An online plug-and-play algorithm for regularized image reconstruction. *IEEE Transactions on Computational Imaging*, 5(3):395–408, 2019.
- [183] Tolga Tasdizen. Principal neighborhood dictionaries for nonlocal means image denoising. *IEEE Transactions on Image Processing*, 18(12):2649–2660, 2009.
- [184] Luis Tenorio. *An introduction to data analysis and uncertainty quantification for inverse problems*. SIAM, 2017.
- [185] Chunwei Tian, Yong Xu, Lunke Fei, Junqian Wang, Jie Wen, and Nan Luo. Enhanced cnn for image denoising. *CAAI Transactions on Intelligence Technology*, 4(1):17–23, 2019.
- [186] Tom Tirer and Raja Giryes. Image restoration by iterative denoising and backward projections. *IEEE Transactions on Image Processing*, 28(3):1220–1234, 2019.
- [187] Zongjiang Tu, Chen Jiang, Yu Guan, Jijun Liu, and Qiegen Liu. K-space and image domain collaborative energy-based model for parallel MRI reconstruction. *Magnetic Resonance Imaging*, 99:110–122, 2023.
- [188] Dmitry Ulyanov, Andrea Vedaldi, and Victor Lempitsky. Deep image prior. In *Proceedings of the IEEE conference on computer vision and pattern recognition*, pages 9446–9454, 2018.
- [189] Dave Van Veen, Ajil Jalal, Mahdi Soltanolkotabi, Eric Price, Sriram Vishwanath, and Alexandros G Dimakis. Compressed sensing with deep image prior and learned regularization. *arXiv preprint arXiv:1806.06438*, 2018.
- [190] Singanallur V. Venkatakrishnan, Charles A. Bouman, and Brendt Wohlberg. Plug-and-play priors for model based reconstruction. In *2013 IEEE Global Conference on Signal and Information Processing*, pages 945–948, 2013.
- [191] Cédric Villani et al. *Optimal transport: old and new*, volume 338. Springer, 2009.
- [192] Pascal Vincent. A connection between score matching and denoising autoencoders. *Neural Computation*, 23(7):1661–1674, 2011.
- [193] Zhangyang Wang, Qing Ling, and Thomas Huang. Learning deep l0 encoders. *Proceedings of the AAAI Conference on Artificial Intelligence*, 30(1), 2016.
- [194] Jay Whang, Erik Lindgren, and Alex Dimakis. Composing normalizing flows for inverse problems. In Marina Meila and Tong Zhang, editors, *Proceedings of the 38th International Conference on Machine Learning*, volume 139 of *Proceedings of Machine Learning Research*, pages 11158–11169. PMLR, 2021.
- [195] Christina Winkler, Daniel Worrall, Emiel Hoogeboom, and Max Welling. Learning likelihoods with conditional normalizing flows. *arXiv preprint arXiv:1912.00042*, 2019.
- [196] Zihui Wu, Yu Sun, Jiaming Liu, and Ulugbek Kamilov. Online regularization by denoising with applications to phase retrieval. In *Proceedings of the IEEE/CVF International Conference on Computer Vision (ICCV) Workshops*, 2019.

- [197] Jinxi Xiang, Yonggui Dong, and Yunjie Yang. Fista-net: Learning a fast iterative shrinkage thresholding network for inverse problems in imaging. *IEEE Transactions on Medical Imaging*, 40(5):1329–1339, 2021.
- [198] Guang Yang, Simiao Yu, Hao Dong, Greg Slabaugh, Pier Luigi Dragotti, Xujiang Ye, Fangde Liu, Simon Arridge, Jennifer Keegan, Yike Guo, and David Firmin. Dagan: Deep de-aliasing generative adversarial networks for fast compressed sensing MRI reconstruction. *IEEE Transactions on Medical Imaging*, 37(6):1310–1321, 2018.
- [199] Qingsong Yang, Pingkun Yan, Yanbo Zhang, Hengyong Yu, Yongyi Shi, Xuanqin Mou, Mannudeep K. Kalra, Yi Zhang, Ling Sun, and Ge Wang. Low-dose ct image denoising using a generative adversarial network with wasserstein distance and perceptual loss. *IEEE Transactions on Medical Imaging*, 37(6):1348–1357, 2018.
- [200] Yan Yang, Jian Sun, Huibin Li, and Zongben Xu. Deep admm-net for compressive sensing MRI. In D. Lee, M. Sugiyama, U. Luxburg, I. Guyon, and R. Garnett, editors, *Advances in Neural Information Processing Systems*, volume 29. Curran Associates, Inc., 2016.
- [201] Yan Yang, Jian Sun, Huibin Li, and Zongben Xu. Admm-csnet: A deep learning approach for image compressive sensing. *IEEE Transactions on Pattern Analysis and Machine Intelligence*, 42(3):521–538, 2020.
- [202] Dong Hye Ye, Somesh Srivastava, Jean-Baptiste Thibault, Ken Sauer, and Charles Bouman. Deep residual learning for model-based iterative ct reconstruction using plug-and-play framework. In *2018 IEEE International Conference on Acoustics, Speech and Signal Processing (ICASSP)*, pages 6668–6672, 2018.
- [203] Raymond A. Yeh, Chen Chen, Teck Yian Lim, Alexander G. Schwing, Mark Hasegawa-Johnson, and Minh N. Do. Semantic image inpainting with deep generative models. In *Proceedings of the IEEE Conference on Computer Vision and Pattern Recognition (CVPR)*, 2017.
- [204] Jaejun Yoo, Kyong Hwan Jin, Harshit Gupta, Jerome Yerly, Matthias Stuber, and Michael Unser. Time-dependent deep image prior for dynamic MRI. *IEEE Transactions on Medical Imaging*, 40(12):3337–3348, 2021.
- [205] Chenyu You, Guang Li, Yi Zhang, Xiaoliu Zhang, Hongming Shan, Mengzhou Li, Shenghong Ju, Zhen Zhao, Zhuiyang Zhang, Wenxiang Cong, Michael W. Vannier, Punam K. Saha, Eric A. Hoffman, and Ge Wang. Ct super-resolution gan constrained by the identical, residual, and cycle learning ensemble (gan-circle). *IEEE Transactions on Medical Imaging*, 39(1):188–203, 2020.
- [206] Martin Zach, Florian Knoll, and Thomas Pock. Stable deep MRI reconstruction using generative priors. *IEEE Transactions on Medical Imaging*, pages 1–1, 2023.
- [207] Martin Zach, Erich Kobler, and Thomas Pock. Computed tomography reconstruction using generative energy-based priors. *arXiv preprint arXiv:2203.12658*, 2022.
- [208] Martin Zach, Thomas Pock, Erich Kobler, and Antonin Chambolle. Explicit diffusion of gaussian mixture model based image priors. In Luca Calatroni, Marco Donatelli, Serena Morigi, Marco Prato, and Matteo Santacesaria, editors, *Scale Space and Variational Methods in Computer Vision*, pages 3–15, Cham, 2023. Springer International Publishing.
- [209] Hai-Miao Zhang and Bin Dong. A review on deep learning in medical image reconstruction. *Journal of the Operations Research Society of China*, 8:311–340, 2020.
- [210] Jian Zhang and Bernard Ghanem. Ista-net: Interpretable optimization-inspired deep network for image compressive sensing. In *Proceedings of the IEEE Conference on Computer Vision and Pattern Recognition (CVPR)*, 2018.
- [211] Kai Zhang, Yawei Li, Wangmeng Zuo, Lei Zhang, Luc Van Gool, and Radu Timofte. Plug-and-play image restoration with deep denoiser prior. *IEEE Transactions on Pattern Analysis and Machine Intelligence*, 44(10):6360–6376, 2022.
- [212] Kai Zhang, Wangmeng Zuo, Yunjin Chen, Deyu Meng, and Lei Zhang. Beyond a gaussian denoiser: Residual learning of deep cnn for image denoising. *IEEE Transactions on Image Processing*, 26(7):3142–3155, 2017.

- [213] Kai Zhang, Wangmeng Zuo, Shuhang Gu, and Lei Zhang. Learning deep cnn denoiser prior for image restoration. In *Proceedings of the IEEE Conference on Computer Vision and Pattern Recognition (CVPR)*, 2017.
- [214] Yulun Zhang, Yapeng Tian, Yu Kong, Bineng Zhong, and Yun Fu. Residual dense network for image restoration. *IEEE Transactions on Pattern Analysis and Machine Intelligence*, 43(7):2480–2495, 2021.
- [215] Bo Zhu, Jeremiah Z. Liu, Stephen F. Cauley, Bruce R. Rosen, and Matthew S. Rosen. Image reconstruction by domain-transform manifold learning. *Nature*, 555(7697):487–492, 2018.
- [216] Daniel Zoran and Yair Weiss. From learning models of natural image patches to whole image restoration. In *2011 International Conference on Computer Vision*, pages 479–486, 2011.